PEAK TO AVERAGE POWER RATIO REDUCTION OF ORTHOGONAL FREQUENCY DIVISION MULTIPLEXING SYSTEM USING TONE INJECTION WITH SIMULATED ANNEALING ALGORITHM AND IMPLEMENTATION ON A SOFTWARE DEFINED RADIO SYSTEM

A DOCTOR OF PHILOSOPHY (PhD) THESIS

in

Modeling and Design of Engineering Systems (MODES)

(Main Field of Study: Electrical and Electronics Engineering)

Atılım University

by

ERDEM ÖZYURT

JULY 2016

PEAK TO AVERAGE POWER RATIO REDUCTION OF ORTHOGONAL FREQUENCY DIVISION MULTIPLEXING SYSTEM USING TONE INJECTION WITH SIMULATED ANNEALING ALGORITHM AND IMPLEMENTATION ON A SOFTWARE DEFINED RADIO SYSTEM

A THESIS SUBMITTED TO
THE GRADUATE SCHOOL OF NATURAL AND APPLIED SCIENCES
OF
ATILIM UNIVERSITY
BY

ERDEM ÖZYURT

IN PARTIAL FULFILLMENT OF THE REQUIREMENTS FOR THE DEGREE OF
DOCTOR OF PHILOSOPHY
IN
MODELING AND DESIGN OF ENGINEERING SYTEMS (MODES) PHD PROGRAM
(MAIN FIELD OF STUDY: ELECTRICAL AND ELECTRONICS ENGINEERING)

JULY 2016

Approval of the Graduate School of Natural and Applied Sciences, Atılım University.

_____

Prof. Dr. İbrahim AKMAN
Director

I certify that this thesis satisfies all the requirements as a thesis for the degree of Doctor of Philosophy.

_____

Prof. Dr. Abdulkadir ERDEN
Program Chair

This is to certify that we have read the thesis "Peak to Average Power Ratio Reduction of Orthogonal Frequency Division Multiplexing System Using Tone Injection with Simulated Annealing Algorithm and Implementation on a Software Defined Radio System" submitted by "Erdem Özyurt" and that in our opinion it is fully adequate, in scope and quality, as a thesis for the degree of Doctor of Philosophy.

_____	_____
Assoc. Prof. Dr. Reşat Özgür DORUK	Prof. Dr. Ramazan AYDIN
Co-Supervisor	Supervisor

Examining Committee Members

Prof. Dr. Şimşek DEMİR	_____
Asst. Prof. Dr. Aykut KALAYCIOĞLU	_____
Prof. Dr. Ramazan AYDIN	_____
Asst. Prof. Dr. Mehmet Efe ÖZBEK	_____
Asst. Prof. Dr. Hakan TORA	_____

Date: 15th of July, 2016

I declare and guarantee that all data, knowledge and information in this document has been obtained, processed and presented in accordance with academic rules and ethical conduct. Based on these rules and conduct, I have fully cited and referenced all material and results that are not original to this work.

Erdem Özyurt

Signature:

ABSTRACT

PEAK TO AVERAGE POWER RATIO REDUCTION OF ORTHOGONAL FREQUENCY DIVISION MULTIPLEXING SYSTEM USING TONE INJECTION WITH SIMULATED ANNEALING ALGORITHM AND IMPLEMENTATION ON A SOFTWARE DEFINED RADIO SYSTEM

Özyurt, Erdem

PhD in Modeling and Design of Engineering Systems (MODES)

Supervisor: Prof. Dr. Ramazan AYDIN

Co-Supervisor: Assoc. Prof. Dr. Reşat Özgür Doruk

July 2016, 73 pages.

Orthogonal frequency-division multiplexing (OFDM) is a popular wideband multicarrier communication technique and resistive to inter-symbol interference and inter-carrier interference however because of signal's high Peak to Average Power Ratio (PAPR), efficiency is degraded because of nonlinear distortion. In this study, Tone Injection technique is used with Simulated Annealing optimization algorithm in order to decrease signal's PAPR with different number of tones and inner threshold is used to decrease necessary number of iterations. Simulation results are compared with other techniques and depict that proposed technique can be used for reducing PAPR of OFDM systems. Designed system is performed on a Software Defined Radio system and using measurements it is shown that nonlinear distortion effect is decreased.

Keywords: OFDM, PAPR Reduction, Tone Injection, Simulated Annealing, Software Defined Radio.

ÖZ

DİKGEN FREKANS-BÖLMELİ ÇOĞULLAMA SİSTEMİNİN TEPE ORTALAMA GÜÇ ORANINI TON ENJEKSİYONU İLE BENZETİMSEL TAVLAMA ALGORİTMASI KULLANARAK DÜŞÜRÜLMESİ VE BİR YAZILIM TANIMLI RADYO SİSTEMİ ÜZERİNDE UYGULAMASI

Özyurt, Erdem

Doktora, Mühendislik Sistemlerinin Modellenmesi ve Tasarımı

Tez Yöneticisi: Prof. Dr. Ramazan Aydın

Ortak Tez Yöneticisi: Doç. Dr. Reşat Özgür Doruk

Temmuz 2016, 73 sayfa

Dikgen frekans-bölmeli çoğullama (OFDM) popüler bir geniş-bant çok taşıyıcılı haberleşme tekniğidir; semboller arası ve taşıyıcılar arası girişime karşı dirençlidir, bununla birlikte işaretin yüksek Tepe Ortalama Güç Oranı'na (PAPR) sahip olması nedeniyle doğrusal olmayan bozulmalar sonucu sistem verimini düşürmektedir. Bu çalışmada, farklı ton sayılarına sahip işaretlerin PAPR değerini düşürmek için benzetimsel tavlama optimizasyon algoritması ile ton enjeksiyonu tekniği kullanılmıştır ve gerekli olan iterasyon sayısını azaltmak için iç eşik değeri kullanılmıştır. Benzetim sonuçları diğer teknikler ile karşılaştırılmış ve önerilen tekniğin OFDM sistemlerinin PAPR değerlerini düşürmek için kullanılabileceği görülmüştür. Tasarlanan sistem Yazılım Tanımlı Radyo (SDR) üzerinde uygulanmış ve ölçümler sonucunda doğrusal olmayan etkilerin azaltıldığı gösterilmiştir.

Anahtar Kelimeler: Dikgen Frekans-Bölmeli Çoğullama (OFDM), Tepe Ortalama Güç Oranı'na (PAPR) düşürme, Ton Enjeksiyonu, Benzetimsel Tavlama, Yazılım Tanımlı Radyo (SDR)

To My Family and My Wife

ACKNOWLEDGEMENTS

I would like to thank my supervisor Dr. Ramazan Aydın and co-supervisor Dr. Reşat Özgür Doruk for their supports. I would also want to thank to my examining committee members Dr. Şimşek Demir, Dr. Aykut Kalaycıoğlu, Dr. Mehmet Efe Özbek and Dr. Hakan TORA for evaluating my research and being in my thesis committee.

I would like to express my deepest gratitude to my previous supervisor and co-supervisor, Dr. A. Çağrı Yapıcı and Dr. Fatma Çalışkan, for their endless encouragement, guidance, and support in my research.

Finally, I wish to thank my family and my wife, who have been with me since the beginning of my studies and have supported me throughout.

I would like to thank to ATÜ-BAP-A-1213-07 project and "TUBİTAK 2211 Yurt İçi Lisansüstü Burs Programı" which supported this thesis.

TABLE OF CONTENTS

LIST OF TABLES

TABLES

LIST OF FIGURES

FIGURES

LIST OF ABBREVIATIONS

ACI	-	Adjacent Channel Interference
ACPR	-	Adjacent Channel Power Ratio
ADC	-	Analog to Digital Converters
BER	-	Bit Error Rate
CP	-	Cyclic Prefix
CCDF	-	Complementary Cumulative Distribution Function
DAC	-	Digital to Analog Converters
DFT	-	Discrete Fourier Transform
dB	-	Decibel
dBc	-	Decibels Relative to The Carrier
dBm	-	Decibel-Milliwatts
dBW	-	Decibel Watt
IFFT	-	Fast Fourier Transform
FEC	-	Forward Error Correction
FPGA	-	Field Programmable Gate Arrays
FDM	-	Frequency Division Multiplexing
ICI	-	Inter-Carrier Interference
ISI	-	Inter-Symbol Interference
IMD	-	Intermodulation Distortion
IDFT	-	Inverse Discrete Fourier Transform
IFFT	-	Inverse Fast Fourier Transform
LNA	-	Low Noise Amplifiers
OFDM	-	Orthogonal Frequency-Division Multiplexing
PA	-	Power Amplifiers
PAPR	-	Peak to Average Power Ratio
PSK	-	Phase-Shift Keying
QAM	-	Quadrature Amplitude Modulation
SA	-	Simulated Annealing
SDR	-	Software Defined Radio
TI	-	Tone Injection
ZP	-	Zero Padding

CHAPTER 1

INTRODUCTION

Communication is essential and necessary for our continuously developing civilization and day by day its importance increases. Communication capability is added to more devices used in our daily life. These devices require communication in higher data rate transfers compared to past, and it is expected that in the future they will require more. As a result, the efficiency of the communication technique becomes important. For efficient higher data rate transfer, multicarrier or wideband communication techniques are preferred instead of single carrier communication techniques.

Orthogonal frequency-division multiplexing (OFDM) is efficient in higher frequencies and it is a multi-carrier modulation technique [1-3]. This technique separates high speed data flows into lower speed, orthogonal and equally spaced multi-carrier sub-channels with the nature of Fourier Transform (FT). After applying Inverse Fourier Transform (IFT) and adding guard bands, communication with OFDM becomes resistive to inter-symbol interference (ISI) and inter-carrier interference (ICI). It also has spectral efficiency and cost effectiveness [1-3]. Due to these advantages, it is employed in several standards and systems for different users and purposes such as Digital Audio Broadcasting (DAB) [4], Digital Video Broadcasting (DVB) [5], Wireless LAN [6], WiMAX [7], ADSL [8], LTE and LTE Advance 4G [9] with the same basis of signal creation. Most important drawback of OFDM system is high peak-

to-average power ratio (PAPR) because of the envelope fluctuation exists for standards and systems, which use OFDM [1-3].

In modern communication systems, several nonlinear components have to be used such as analog to digital converters (ADC), digital to analog converters (DAC), mixers, power amplifiers (PA), low noise amplifiers (LNA). These components cause nonlinear distortion in both out of band and in band. Nonlinear distortion affects the system by compressing fundamental components, increasing co-channel and adjacent channel interference, and spectral regrowth. These effects are increased due to PAPR and reduces OFDM systems performances dramatically [11,12]. Nonlinear distortion also reduces power efficiency of the system. Ordinary OFDM systems utilize the back-off power to eliminate these problems and fit the regulator's spectrum mask. However utilizing back-off power decreases the efficiency of PA. In order to solve this issue, linearization techniques for PA are proposed such as feedback [12,13], feedforward [14,15] and predistortion [16-18]. These techniques are dependent on the type of PA and cannot be used in different systems and also they are dealing with only the PA's distortion due to nonlinearity rather than the whole system's distortion. Another approach is to reduce PAPR of symbol to decrease nonlinear distortions and to enhance efficiency of the system. Several techniques are proposed to reduce PAPR such as Clipping [19,20], Nonlinear Companding Transform (NCT) [21,22], Tone Reservation (TR) [23,24], Tone Injection (TI) [24-31], Partial Transmission Sequence (PTS) [32-38], Selective Mapping (SLM) [39,40], Constellation Extension [41,42] and etc. Except Tone Injection, all these techniques either need side information, reduce transmission rate or corrupt the signal.

TI technique is based on changing appropriate part of the OFDM signal with extended mapping constellation. Since there exists excessive amount of possibilities, process becomes combinatorial optimization problem. To decide which part is to be changed, an optimization algorithm is used to find the minimums of OFDM symbol. Researchers used Greedy algorithm [24], linear programming [25], parallel stochastic search [26], neural networks [27], genetic algorithm [28], tabu search [29], cross entropy [30] and aggressive clipping [31] methods to find most possible candidate tones in a symbol. Due to FFT operation, PAPR's of the symbol cannot be predicted

by using frequency domain signals or parts of them as optimization algorithms mentioned above.

In this study, Simulated Annealing (SA) is used together with TI as an optimization algorithm. SA algorithm is introduced by Kirkpatrick, Gelatt, and Vecchi [43], and it is used to find global minimum or maximum of a cost function without trapped in local minimums or maximums through probabilistic approach. Using TI and SA is novelty and it can be considered as contribution of this thesis to the literature.

Software Defined Radio (SDR) is described in Wireless Innovation Forum as "Radio in which some or all of the physical layer functions are software defined" where physical layer functions are digital signal processing, analog-digital conversion, radio frequency front end and antennas [45]. With this definition, most of the devices we used in our daily life can be classified as SDR, such as computers, mobile phones, televisions, etc. However, in this thesis, SDR development platforms with multifunction are focused rather than general definition of SDR. By using SDRs, more than one digital communication techniques can be applied at the same time, cognitive radio properties can be added and all these functions can be updated according to requirements. Especially for the developers and researches, it allows to perform communication systems with newer techniques to enhance system performances.

A basic SDR system consists of a signal processor, RF board and amplifier. RF board is controlled with signal processor units and responsible for performing ADC/DAC, up conversion and down conversion operations. For signal processor, General Propose Processors (GPP), Digital Signal Processors (DSP) and Field Programmable Gate Arrays (FPGA) can be used. FPGA is preferred due to its parallel processing capability.

In this study, an OFDM system is developed on SDR, which consists of FPGA, RF board and PA. To reduce the PAPR of OFDM symbol, TI technique and SA optimization algorithm are used together for the first time. The output of the PA is measured both with and without PAPR reduction technique. According to adjacent channel power ratio (ACPR) measurements, proposed PAPR reduction technique is successively decrease nonlinear distortion of the system.

In this thesis, principles of OFDM and PAPR are discussed in Chapter 2. In Chapter 3, memoryless nonlinearity concept is given in a perspective of multitoned inputs. In Chapter 4, PAPR reduction techniques are discussed briefly and applied TI technique and SA algorithm are described. In Chapter 5, basic information about SDR and experimental setup are given. In Chapter 6, simulation and experimental results are given and Chapter 7 concludes thesis.

CHAPTER 2

ORTHOGONAL FREQUENCY-DIVISION MULTIPLEXING

2.1 Introduction

Today, demands on data transmission rates are increasing, and with respect to these demands, modern communication techniques are compiled to transfer more data efficiently. Multicarrier or wideband communication techniques are preferred instead of single carrier communication techniques and these techniques provide higher data transfer rate. OFDM is one of these techniques. OFDM takes part in modern communication due to its immunity to multipath propagation problems, spectral efficiency and cost effectiveness. It is used in several standards and systems such as DAB [4], DVB [5], Wireless LAN [6], WiMAX [7], ADSL [8], LTE and LTE Advance 4G [9]. Although intended usage is varied, OFDM's biggest challenge is nonlinear distortion due to high PAPR.

In this chapter, basics of conventional single carrier and multicarrier techniques are given in Section 2. In Section 3, principles of OFDM are discussed and in Section 4, measurement and distribution of PAPR are given.

2.2 Conventional Single Carrier and Multicarrier Techniques

Ordinary single carrier communication techniques carry limited data and the quality is dependent on channel conditions. In wireless communication, transmitted signals may arrive to receiver from different paths because of multipath propagation, which is

dominant on the performance of single carrier communication. Equalization that is utilized by finite impulse response (FIR) filters is used to tolerate the multipath propagation. Channel bandwidth is proportional to data rate. While data rate increases, required bandwidth overflows coherence bandwidth, which is end up with ISI distortion due to multipath propagation as seen in Figure 2.1. As a result, excessive equalization tabs are needed and these tabs increase implementation complexity of communication systems.

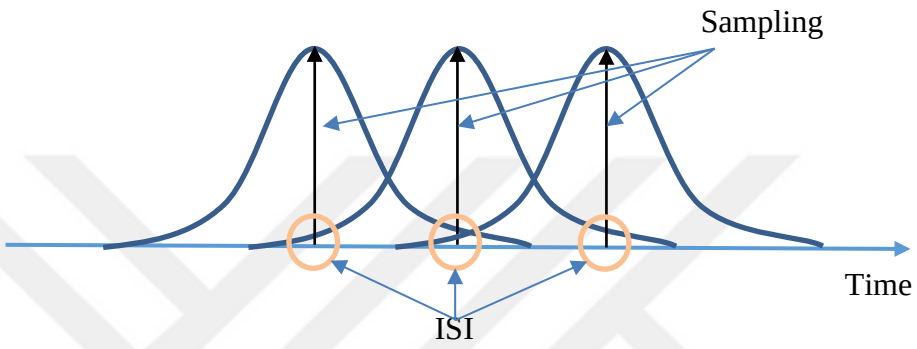

Figure 2.1. ISI distortion

Multicarrier techniques are introduced to communicate with higher data rates with respect to single carrier techniques. In frequency division multiplexing (FDM) technique which is a basic multicarrier modulation technique, each subcarrier is separated from others with guard bands to eliminate ISI and ICI as seen in Figure 2.2.(a). Size of guard bands is related to delay spread, which is dependent on frequency and environment. According to delay spread measurements which were carried out indoor environments, median values of these measurements vary between 25-106 ns and maximum values are between 30-270 ns for frequencies between 1.8-2.4 GHz [45,46].

2.3 Principles of OFDM

Weinstein and Ebert proposed to create linearly independent i.e. orthogonal subcarriers to place them closer to adjacent ones as seen in Figure 2.2.(b) by using Inverse Discrete Fourier Transform (IDFT) in transmitter and Discrete Fourier Transform (DFT) in receiver [47]. Each subcarrier is orthogonal to each other rather

than classical parallel data system and as a result, crosstalk between subcarriers is prevented.

OFDM can be classified as both digital modulation and multiplexing technique and frequency division multiplexing is carried out using DFT rather than using filtering operation in FDM. An OFDM signal consists of multiple subcarriers, which are mapped to complex symbols by using digital modulation techniques such as phase-shift keying (PSK) or quadrature amplitude modulation (QAM) as given in Eq. 2.1.

$$x[n] = \frac{1}{\sqrt{N}} \sum_{k=0}^{N-1} X_k e^{j2\pi kn/N} \quad n = 0, .., N \tag{2.1}$$

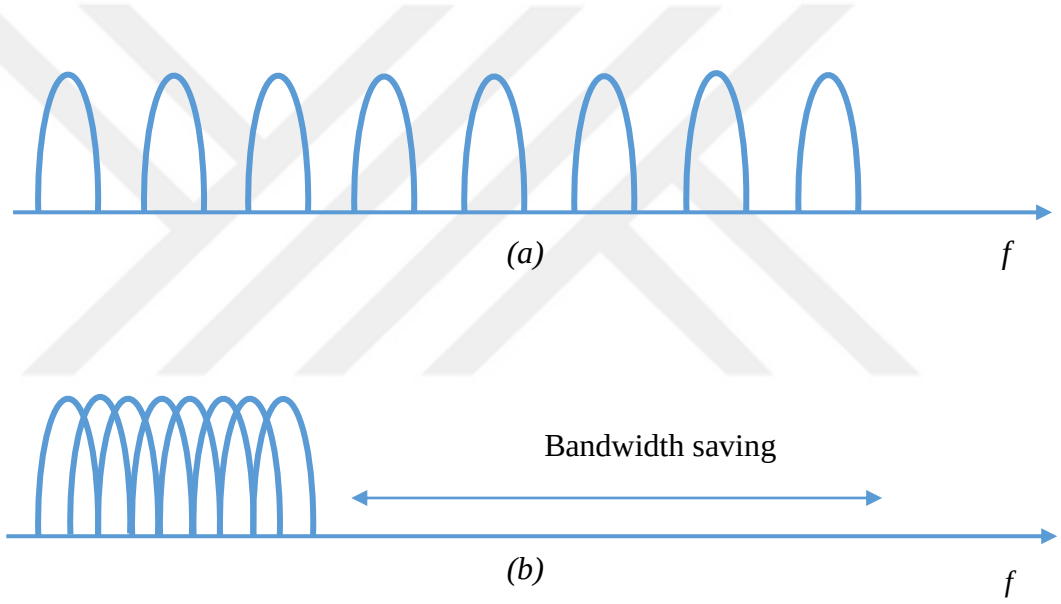

Figure 2.2. (a) FMD and (b) OFDM spectrums

The separation between subcarriers is $\Delta f = 1/T_s$, where T_s is OFDM symbol duration and each subcarrier has integer number of oscillation in T_s duration. In Figure 2.3, time domain representations of four subcarriers are given and they have exactly one cycle difference with respect to each other. As seen in the figure, cycling periods of subcarriers are adjusted precisely to obtain orthogonality and to provide spectral efficiency.

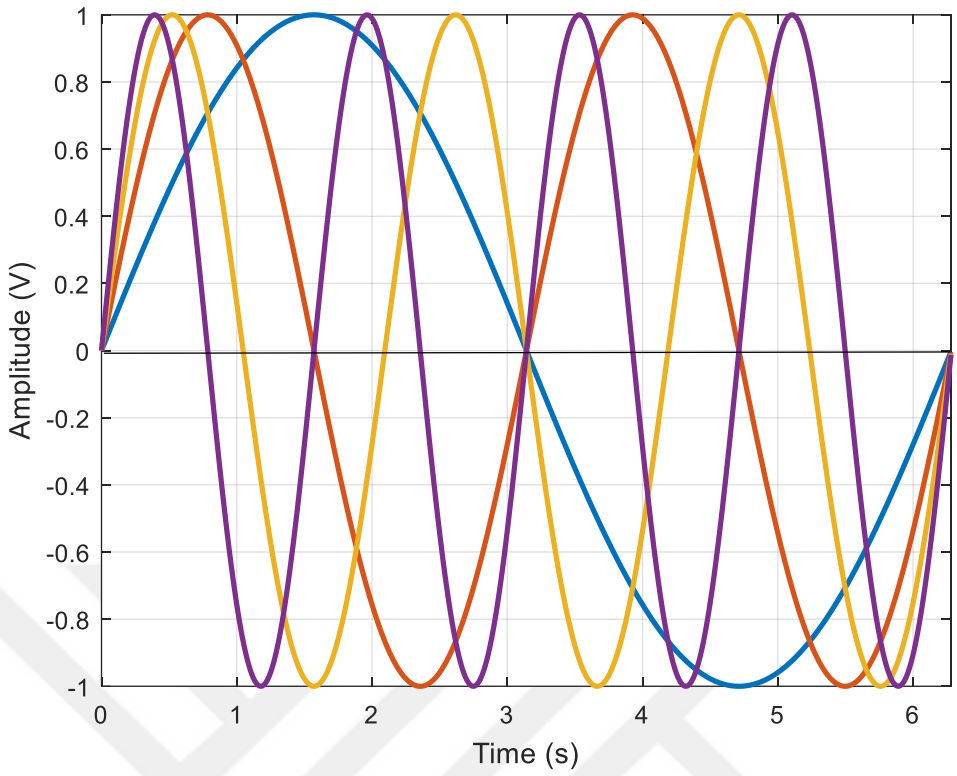

Figure 2.3. Four subcarrier's time domain representation

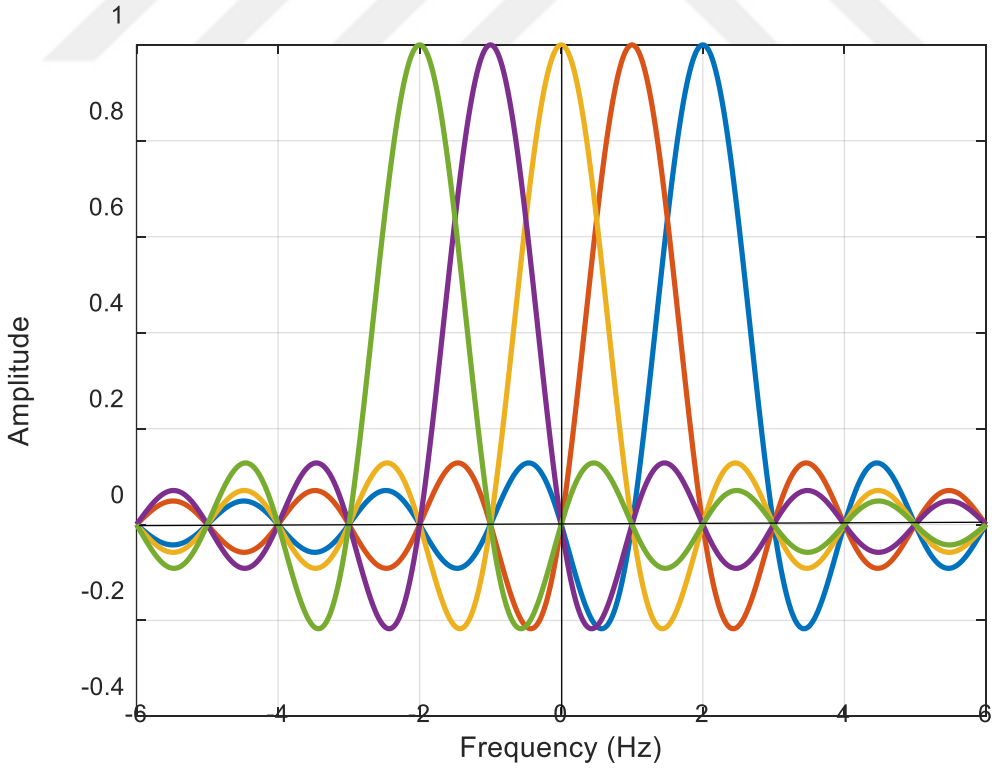

Figure 2.4. Spectral represantation of five subcarriers

With convolution of dirac delta, shape of each subcarrier assumed as pulse and spectrum becomes a *sinc* function spaced with $\Delta f = 1/T_s$ given in Figure 2.4. As seen in the figure, when subcarrier reaches to its maximum peak power, other subcarriers' powers are zero.

Although OFDM technique decreases bandwidth requirements by compressing subcarriers, only one guard interval between the symbols is adequate to remove ISI effect, not between adjacent subcarriers contrary to FDM. During the design of OFDM systems, parameters such as subcarrier number, guard time, symbol duration, subcarrier spacing, digital modulation type and channel coding type are decided considering the system requirements such as allowable bandwidth, bit rate and tolerable delay spread.

In Figure 2.5, illustration of simple transmitter and receiver OFDM architecture is given. A basic OFDM transmitter has to include symbol mapping, IDFT as OFDM modulator and guard interval insertion operations. Generated symbol is converted to analog signal by using digital to analog conversion block and baseband signal is up converted to bandpass by I/Q modulation and then it is amplified. The signal between mapper and DAC is denoted as parallel data and for the rest, it is denoted as series data. As seen in the figure, opposite of operations in the transmitter are carried out in the receiver. These operations are described below.

a) Channel Coding and Decoding

In channel coding block, forward error correction (FEC) and interleaving operations are carried out. FEC techniques are utilized mostly to decrease errors of transmitting data by using redundant data without retransmitting it. FEC is also used for compressing data or defining redundant data and reduce ICI. As a result of FEC operations, bandwidth of the signal changes. FEC operations do not require using channel coding for some of the OFDM systems and they depend on user requirements and channel characteristics. There are two FEC categories, these are block codes and convolutional codes. Block codes use fixed size of symbols and well known examples are Reed Solomon coding, Hamming Codes and Golay. In convolutional codes, there is variable size of symbols [1].

In communication channels, frequency selective fading is occurred frequently, and part of subcarriers may be affected more than the others. During FEC operations, interleaving randomizes bit errors by separating bits in the symbols in a certain manner and in receiver combines them before the decoding process.

b) Symbol Mapping and Demapping

In OFDM system, digital modulation techniques are used to map group of bits to symbols using methods such as QAM, BPSK, QPSK, etc. QAM is preferred with respect to other techniques since it is easier to implement. In Figure 2.6, constellations of QPSK, 16-QAM and 64-QAM are given without signal normalization. QPSK, 16-QAM and 64-QAM accept 2, 4 and 8 number of bits respectively to map them in both quadrature and inphase axes. As seen in the figure, QPSK maps with 4, 16-QAM maps with 16 and 64-QAM maps with 64 different combinations. The output of QAM is a complex number. In Figure 2.7, gray coded constellation of 16-QAM is given. As seen in the figure, only one bit differs from its neighbor. This is used to decrease bit error rate (BER) of the whole system.

c) IDFT/DFT

IDFT is the most critical operation in OFDM system where it modulates mapped complex symbols by orthogonal subcarrier. This process decreases the complexity of multicarrier systems since using oscillators and filters in conventional multicarrier systems are troublesome. As seen in Figure 2.8, subcarriers are spaced with $1/T_s$, where T_s is the total symbol duration. The orthogonality of subcarriers is proved by using Eq. 2.2. Before IDFT operation, virtual carriers may be added to reduce out of band radiation although this operation reduces the usable subcarrier number.

$$\frac{1}{T_s}\int_0^{T_s} e^{i2\pi f_k t}\, e^{-i2\pi f_n t} dt = \delta_{kn} = \begin{cases} 1, k = n \\ 0, otherwise \end{cases} \qquad (2.2)$$

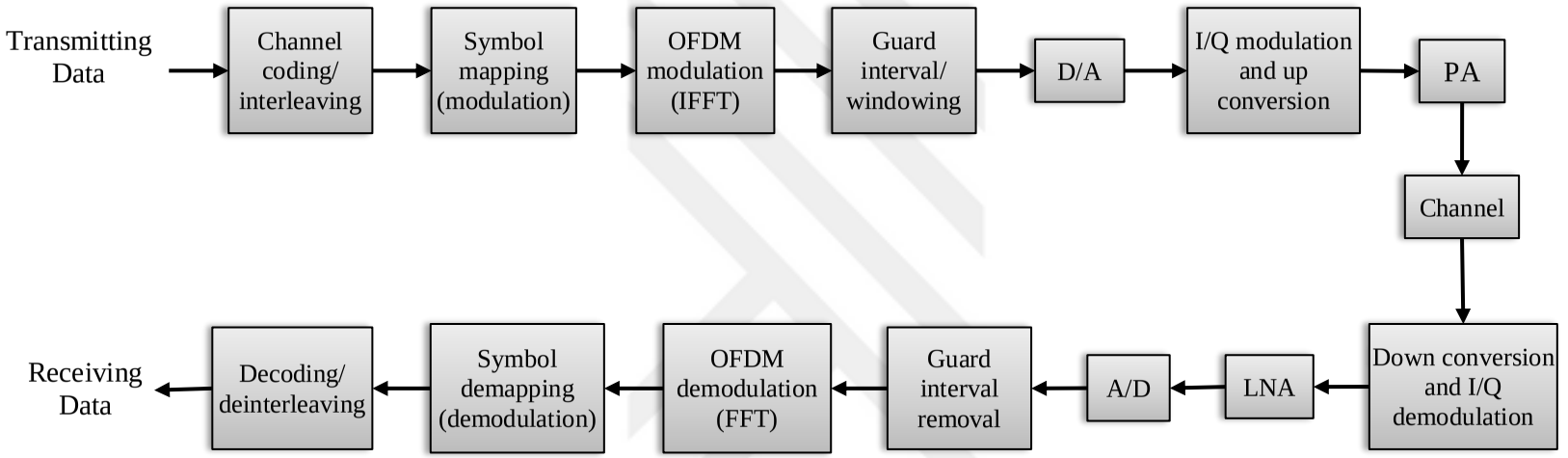

Figure 2.5. Simple OFDM Architecture

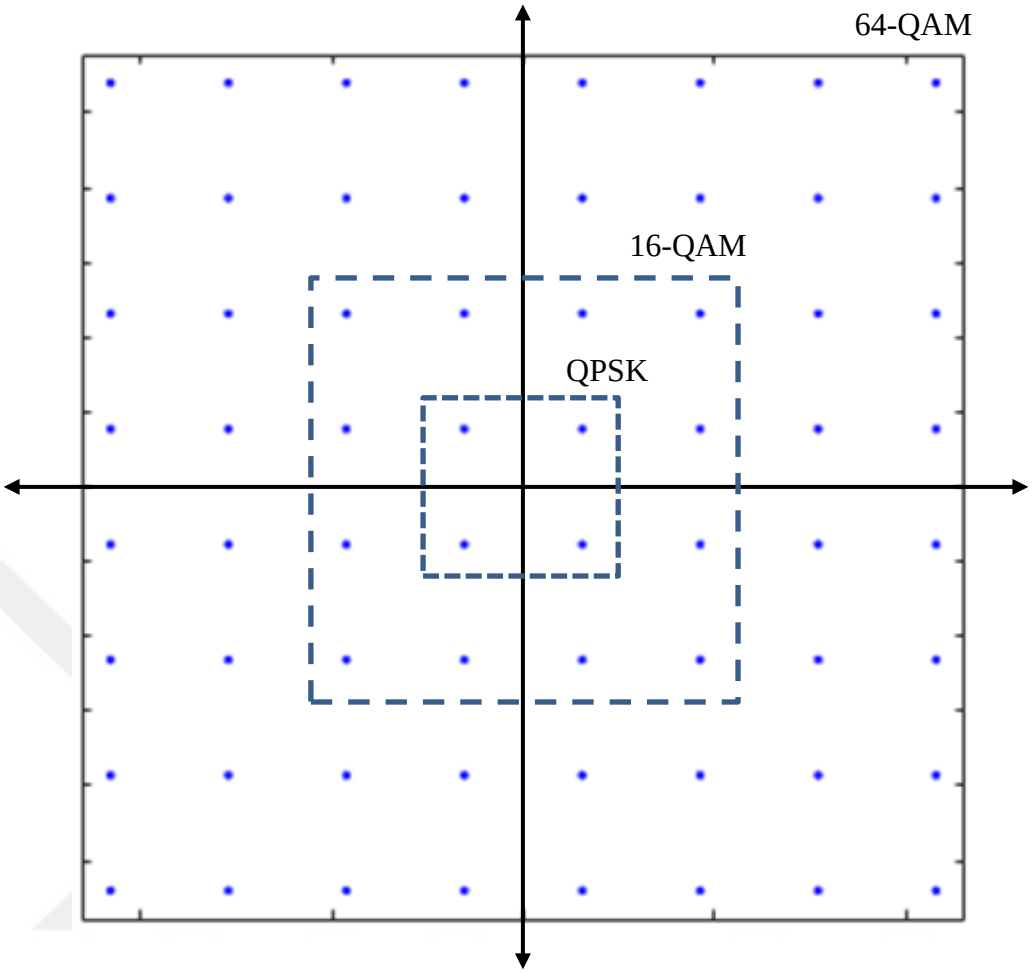

Figure 2.6. Constellation of 64-QAM, 16-QAM and QPSK

IDFT and DFT are time consuming operations for OFDM systems. At every turn, there are N^2 complex multiplication and N^2-N complex additions for N-point IDFT. Embedded systems could be inadequate to perform these operations in real time. Inverse Fast Fourier Transform (IFFT) is introduced to reduce required multiplications. For N-point FFT operations, radix-4 based algorithm requires only $^3/_8 N \log_2(N-2)$ complex multiplications and $N\log_2 N$ complex additions. Number of operations is further decreased using iterative algorithms.

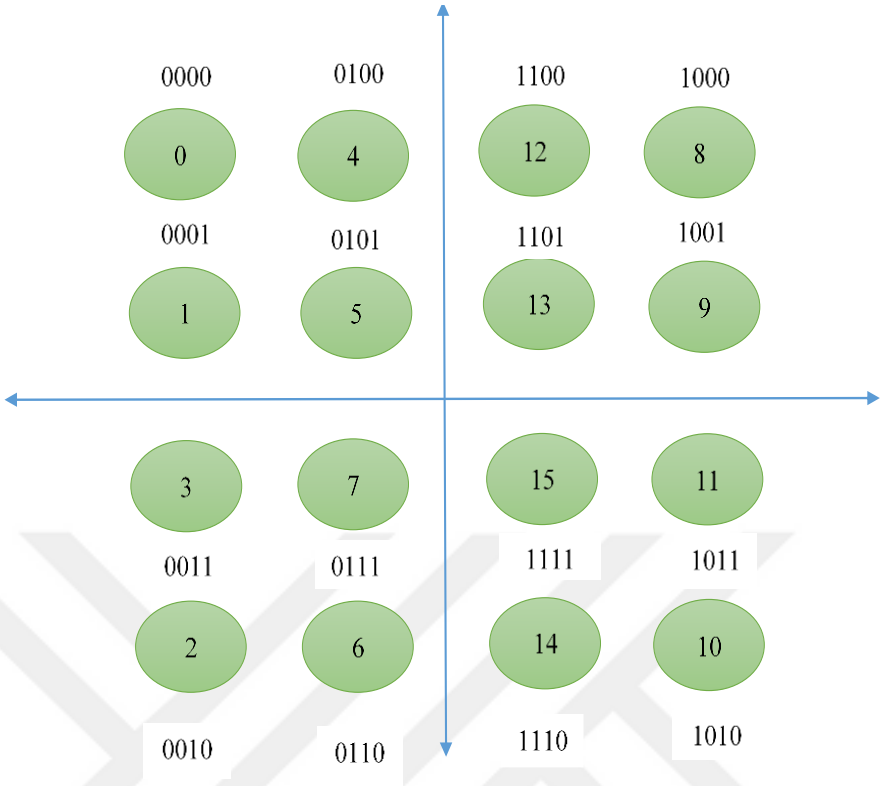

Figure 2.7. Gray coded 16-QAM

d) Guard Interval

To reduce ISI of OFDM symbol, guard intervals are employed. There are two frequently used guard interval types, cyclic prefix (CP) and zero padding (ZP). In CP technique, a portion which is larger than the maximum delay spread of multipath propagation is copied from the lag of the symbol and attached in front of the symbol and an interval greater than maximum delay spread is created as seen in Figure 2.9. Copying beginning of symbol and attaching to the end of it is called cyclic suffix and it is used to avoid interference between streams.

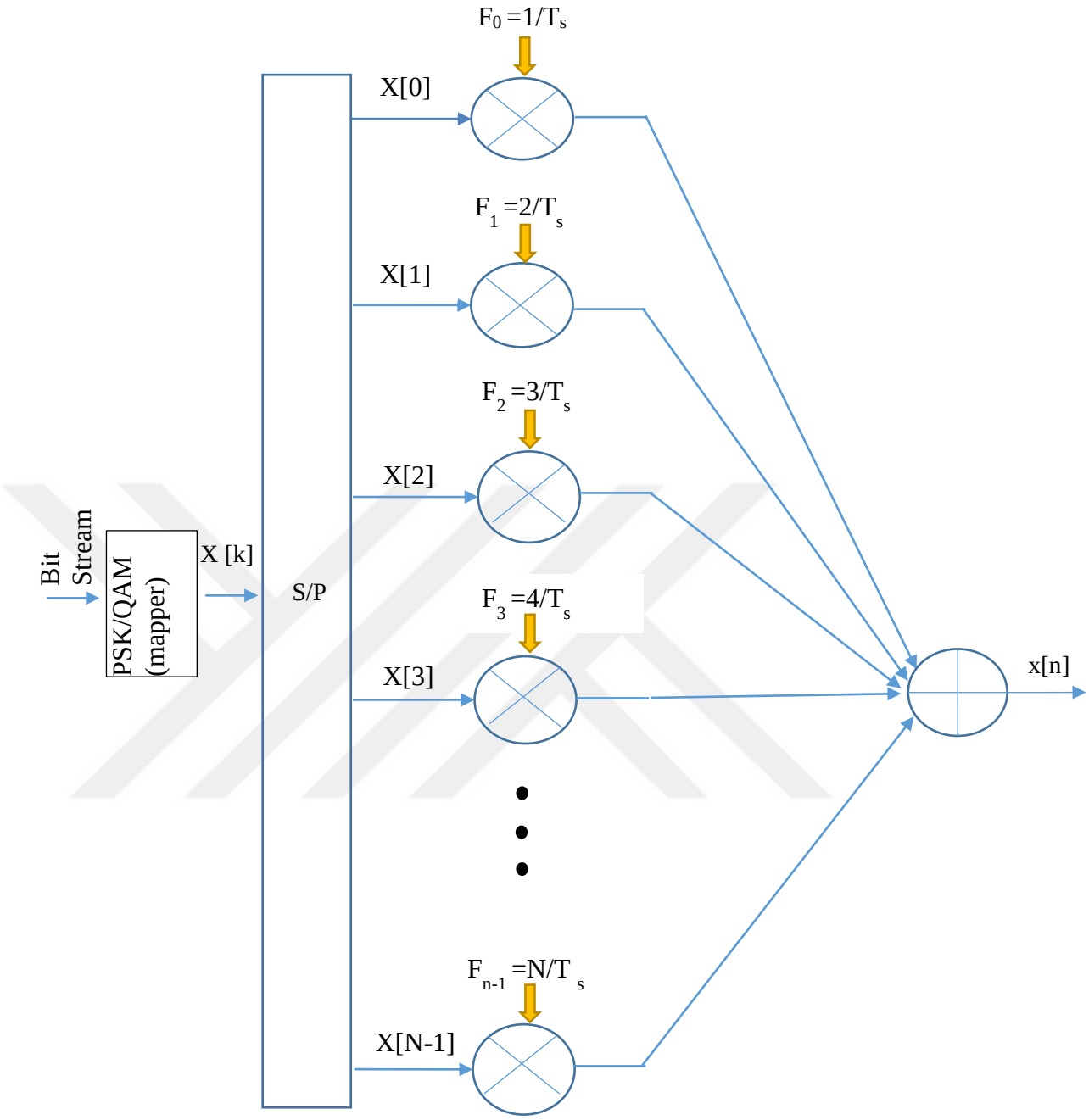

Figure 2.8. OFDM modulation

In ZP technique, zeros with the length of maximum delay spread are placed into the guard interval. This technique also prevents ISI however defining zero subcarriers might cause ICI. ZP employed OFDM symbols have smaller bandwidth than CP employed ones and this ensures more efficient power usage.

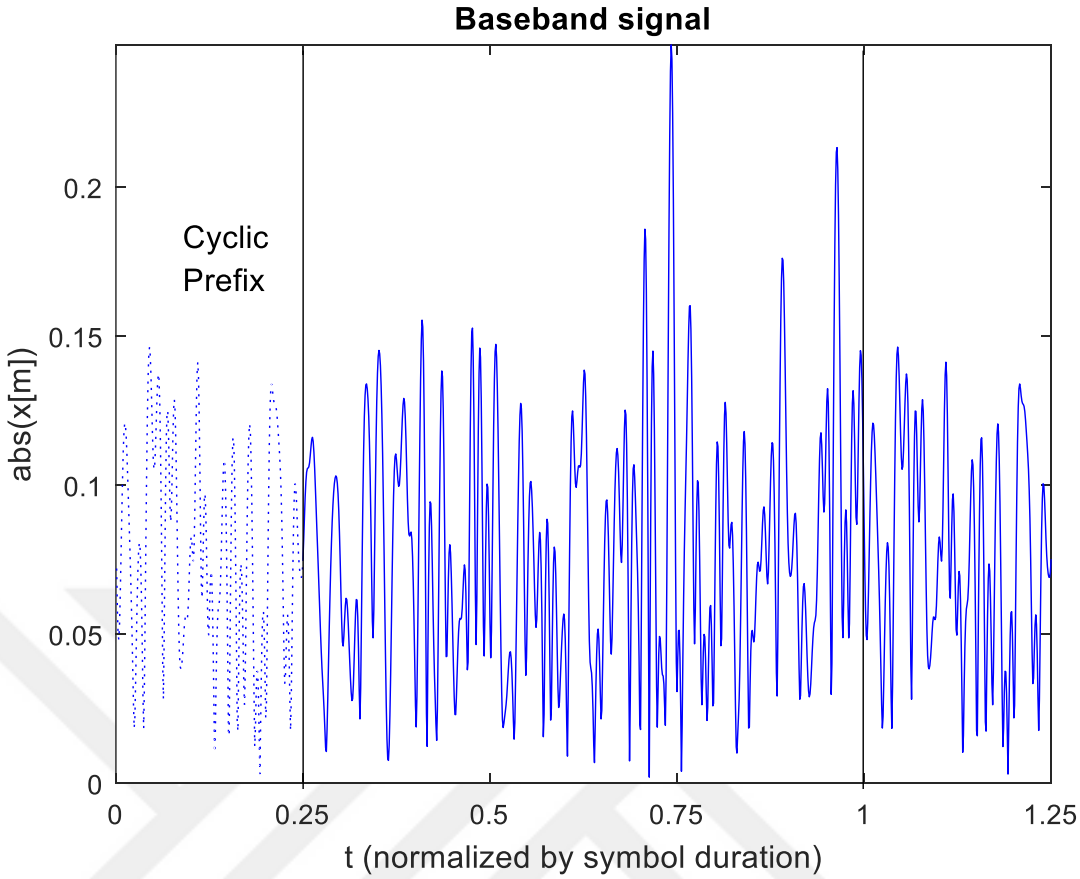

Figure 2.9. Cyclic prefix in an OFDM symbol

e) Windowing

Subcarriers of OFDM have shaped like a sinc function and side lobes of sinc function increase the out of band radiation and adjacent channel interference (ACI). These side lobes could be reduced by filtering operation however filtering adds complexity into system. Windowing operation can reduce side lobes before amplification. Raised cosine windowing is one of the most preferred windowing method and its detail can be seen in Eq. 2.3 [1]

$$w(t) = \begin{cases} 0.5 + 0.5\cos(\pi + \dfrac{\pi}{\beta T_s}), & 0 \le t < \beta T_s \\ 1, & \beta T_s \le t \le T_s \\ 0.5 + 0.5\cos\left(\dfrac{(t - T_s)\pi}{\beta T_s}\right), & T_s < t \le (\beta + 1)T_s \end{cases} \quad (2.3)$$

where β is roll-off factor and T_s is total symbol duration of OFDM symbol including guard intervals as seen in Figure 2.10. The effect of roll-off factor is increased from 0 to 0.1, and as seen Figure 2.11, side lobes of OFDM symbol is drastically decreased.

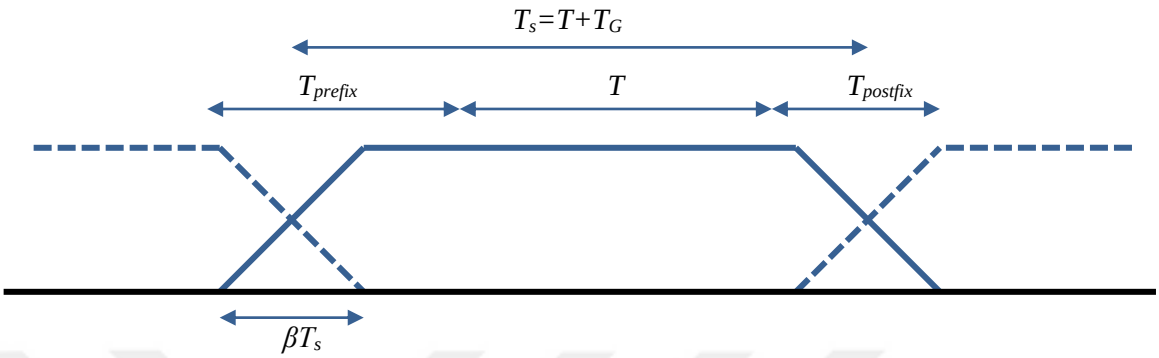

Figure 2.10. OFDM cyclic extension and windowing

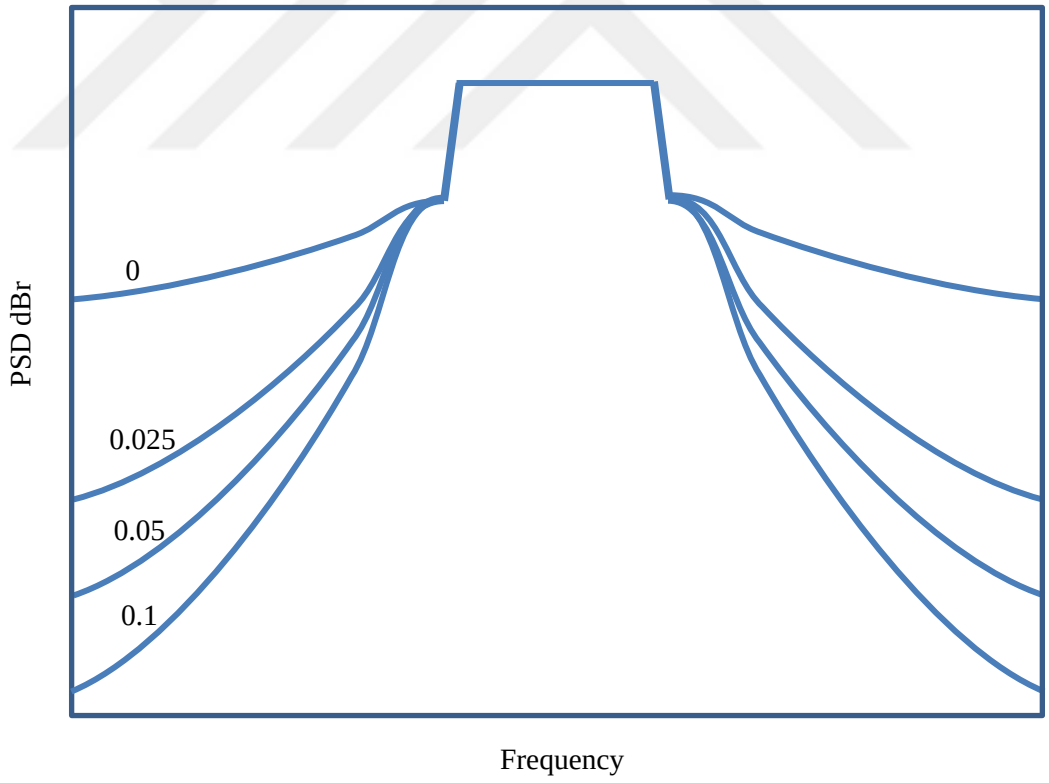

Figure 2.11. Effect of windowing

f) Synchronization

Synchronization in OFDM systems is an important issue as also in modern communication systems. Recovering the data from received data, which is corrupted by the channel and other factors, is critical while the trend is transmitting more data with more OFDM symbols (MIMO OFDM). In OFDM systems, synchronization problems are mostly based on carrier frequency offsets and symbol timing offsets [48-50].

Carrier frequency offsets are caused in down-conversion of OFDM symbol from bandpass signal to baseband signal. Additionally for outdoor applications, Doppler shift also needs to be taken into consideration. Carrier offsets could disturb orthogonality of subcarriers or cause a shift on peaks and these offsets will create totally different data as shown in Figure 12 [49,50].

Defining guard interval between OFDM symbols also reduces symbol timing errors. When the delay spread is less than guard interval, the receiver could lock on the symbol using detection algorithms [49,50].

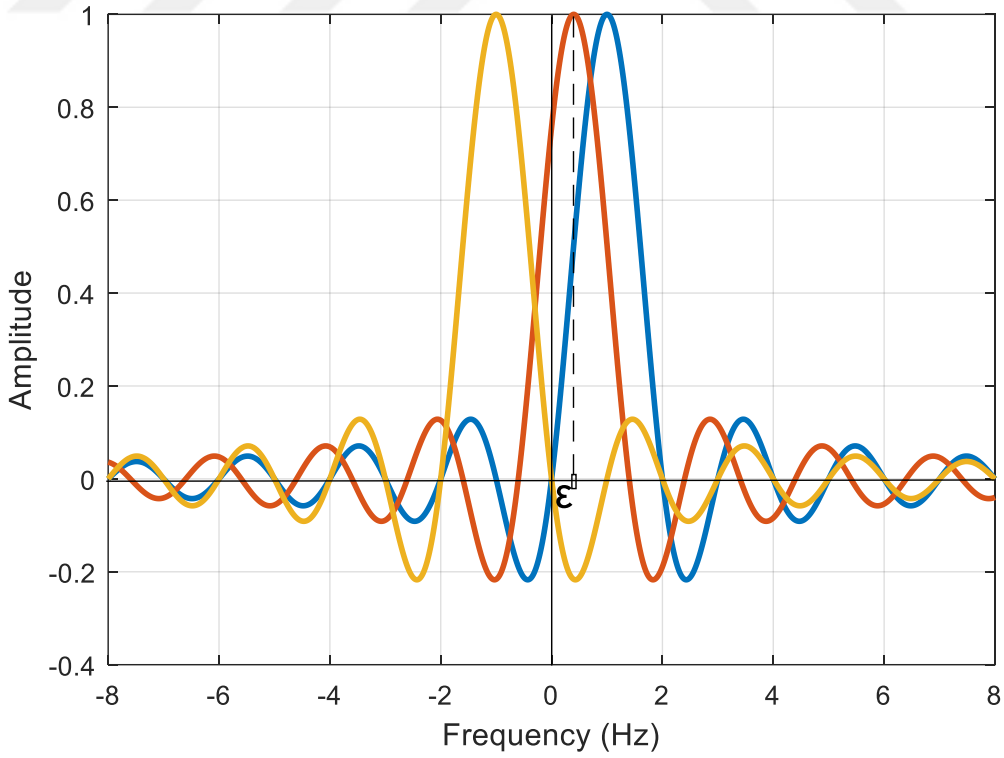

Figure 2.12. Frequency offset of OFDM of subcarriers

2.4 PAPR of OFDM Symbols

a) Definition of PAPR

Signals affect the components in the system and degrade the system performance. They also are more affected by channel conditions. Therefore, it is important to create a signal that will be less affected by outside parameters. To observe the quality of the signal, a parameter such as peak power, average power or PAPR is needed. In OFDM systems, envelope fluctuation i.e. PAPR preserves a meaningful information about the signals even in baseband. PAPR is simply defined as ratio of average power to maximum peak power as Eq. 2.4 for continuous signals.

$$PAPR(x[n]) = \frac{max_n|x(t)|^2}{\frac{1}{NT}\int_{t=0}^{T_s}|x(t)|^2 dt} \quad (2.4)$$

For discrete signals, Eq. 2.4 can be rearranged as given in Eq. 2.5.

$$PAPR(x[n]) = \frac{max_n|x[n]|^2}{\frac{1}{N}\sum_{n=0}^{N-1}|x[n]|^2} \quad (2.5)$$

It has to be noted that, estimating signal parameters from baseband discrete signals could cause reduction in accuracy rather than estimating from continuous signals. As seen in Figure 13, original signal is sampled by two different sampling ratio, *L=1* and *L=4*. When the sampling ratio is chosen as 1, all the peaks are missed. Because of this, while calculating PAPR, *L* has to be chosen at least 4 [51] and Eq. 2.5 can be rewritten as Eq. 2.6.

$$PAPR(x[{}^{n}/_{L}]) = \frac{max_n\left|x[{}^{n}/_{L}]\right|^2}{\frac{1}{NL}\sum_{n=0}^{NL-1}\left|x[{}^{n}/_{L}]\right|^2} \quad (2.6)$$

PAPR of the passband signal is related with baseband signal's PAPR. A passband signal can be defined by using Eq. 2.7

$$x_{PB}(t) = Re\{x(t)\cos(\omega_c t)\} - Im\{x(t)\sin(\omega_c t)\} \quad (2.7)$$

where ω_c is equal to $2\pi f_c$ and f_c is the carrier frequency. Furthermore, the average power of passband signal, which is needed to calculate PAPR as in Eq. 2.6, is half of the baseband signal as seen in Eq. 2.8. This means that, the expected PAPR of passband signal is twofold of baseband signal's PAPR [52]

$$E[|x_{PB}(t)|^2] = \frac{1}{2} E[|x(t)|^2] \tag{2.8}$$

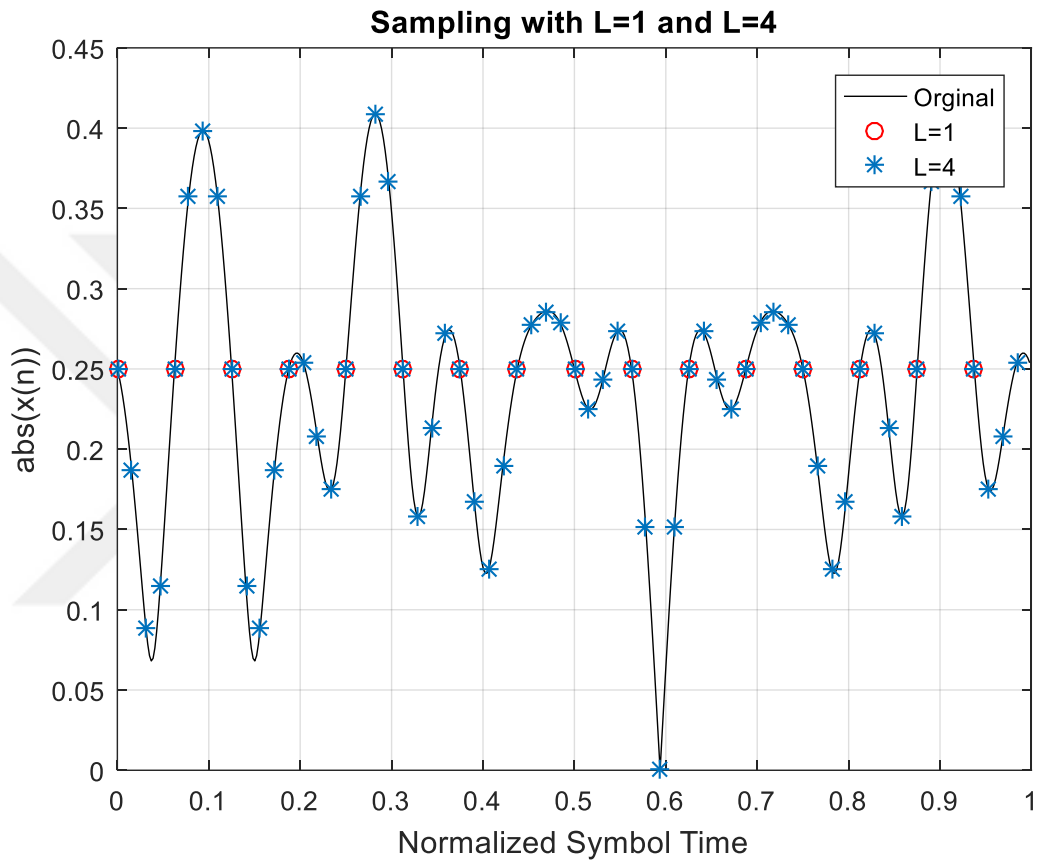

Figure 2.13. Sampling a signal with different ratios

b) Distribution of PAPR

In the system design level, requirements have to be clearly specified especially to minimize distortions. Maximum PAPR of MQAM modulated OFDM symbol is given in [53] with an inequality as Eq. 2.9

$$\frac{3N}{M-1} \leq PAPR_{max}[x(n)] \leq \frac{3N(\sqrt{M}-1)^2}{M-1} \tag{2.9}$$

where N is the number of subcarriers and M is the constellation size of QAM. However, maximum PAPR values do not occur frequently and using large scaled components increases the cost and complexity of the system. To optimize PAPR, Complementary Cumulative Distribution Function (CCDF) is often used. Researcher proposed several CCDF of PAPR depending on the number of subcarriers, N [52,56]. For the low number of subcarriers, CCDF of PAPR can be obtained by Eq. 2.10 with the assumption that PAPR of OFDM signal can be found by Gaussian process and signal has a Rayleigh distribution [54]

$$Prob\{PAPR > \gamma\} = 1 - (1 - e^{-\gamma})^N \qquad (2.10)$$

where γ is the threshold for PAPR. For large number of subcarrier, Eq. 2.10 is revised based on empirical studies as given in Eq. 2.11 [55]

$$Prob\{PAPR > \gamma\} = 1 - (1 - e^{-\gamma})^{\alpha N} \qquad (2.11)$$

where α is fitting factor and it can be found by empirical studies. Since N is chosen in interval between 16 to 2048 in literature, the models diverge from actual values for small N or for large N. A more general CCDF is given in [56] and summarized in [52], based on extreme value theory for Chi-squared-2 processes as in Eq. 2.12

$$Prob\{PAPR > \gamma\} = 1 - exp\left\{-2e^{-\gamma}\sqrt{\frac{\pi\gamma\sum_{k=-K}^{K} K^2{\sigma_k}^2}{\sum_{k=-K}^{K}{\sigma_k}^2}}\right\} \qquad (2.12)$$

where $K=N_{used}/2$ and ${\sigma_k}^2$ is the power of related subcarrier. By using Eq. 2.12, occurrence probability of PAPR, which is greater than the threshold γ, is obtained. Furthermore, CCDF of PAPR can be obtained empirically by using baseband signal with Eq. 2.6 as seen in Figure 2.14. 10^5 randomly generated OFDM symbols consist of modulated 48 subcarriers with 16-QAM, and 16 of them are zero padded subcarriers. As seen in the figure, the probability of symbols greater than 8.3 dB is 0.1, i.e. Pr[PAPR > 8.3]=10^{-1} and for Pr[PAPR > 10.4] the probability equals to 10^{-3}.

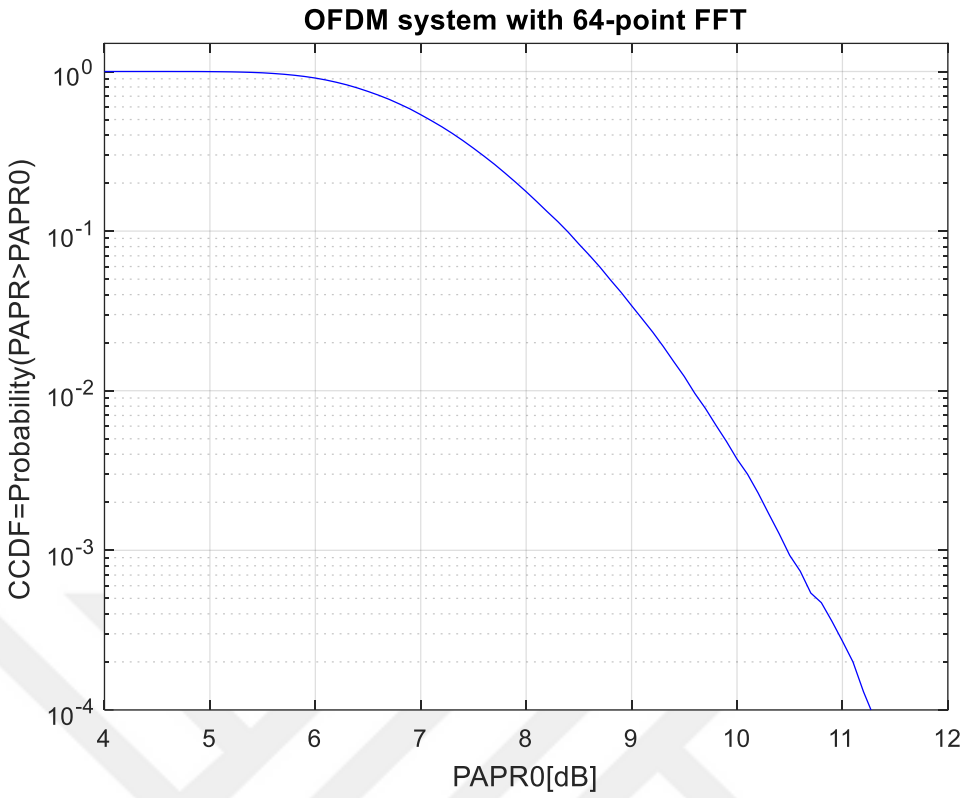

Figure 2.14. Experimentally obtained CCDF of OFDM dymbols

CHAPTER 3

NONLINEARITY IN COMMUNICATION SYSTEMS

3.1 Introduction

Communication systems are affected by several internal and external factors such as signal perturbation, which causes impairments of the system performance. Signal perturbations are originated from two main factors. The first one is additive signals which exist in the system and they are uncorrelated with input and output. Most known example of them is channel noise, which can be also observable when the system is not operating. The second and most challenging one is distortion, which is observable while the system is operating and it can be destructive for both amplitude and phase of the fundamental components of the signal. Distortion sources are divided mainly into two subsections, these are linear and nonlinear systems. Simply, a linear system could be described by using Eq. 3.1. and the superposition of individual inputs as Eq. 3.2 for any *a* and *b* values

$$x_1(t) \rightarrow y_1(t) \quad x_2(t) \rightarrow y_2(t) \tag{3.1}$$

$$ax_1(t) + bx_2(t) \rightarrow ay_1(t) + by_2(t) \tag{3.2}$$

where $x_1(t)$ and $x_2(t)$ represent two different input and $y_1(t)$ and $y_2(t)$ are the corresponding outputs. As seen in Eq. 3.2, if the system is linear then the output is proportional to the input of the system. Furthermore linear distortion components are also proportional to the input and while varying coefficients *a* and *b*, linear distortion

components increase or decrease proportionally to the input. So linear distortion is easily observed.

However, if the system does not satisfy Eq. 3.1 and 3.2, the system is called a nonlinear system. In modern communication systems, several components act as nonlinear such as ADC, mixers and PA in transmitter, DAC and LNA in receivers. Even passive elements such as filters, connectors etc. introduce nonlinear distortion components due to magnetic flux saturation.

The effects of nonlinear distortion occur in both out of band and in band. At the out of band, harmonics of the fundamental frequency are observed and these can be filtered with a bandpass filter operation. However, at in band, reduction in fundamental components, co-channel and adjacent channel interference and spectral regrowth are observed due to nonlinear distortion, which is more destructive than linear distortion especially for multicarrier signals with high envelope fluctuation. For PA's, these effects are observed by input and output power relations. Gain of the amplifier is fundamental output signal's power versus fundamental input signal's power as given in Eq. 3.3 and Figure 3.1. Input signal is amplified using DC power P_{dc} and P_{diss} dissipated power due to nonlinear distortion (harmonics, spectral regrowth, etc.) in addition to heat as given in Eq. 3.4

$$G = \frac{P_{out}}{P_{in}} \tag{3.3}$$

$$P_{out} + P_{diss} = P_{in} + P_{dc} \tag{3.4}$$

A memoryless nonlinear system's input/output relation can be modelled by general power series expression as given in Eq. 3.5

$$y(t) = \sum_{k}^{\infty} a_k x(t)^k \tag{3.5}$$

where *x(t)* is the input, *y(t)* is the output and a_k's are the coefficient of the equation. Depending on the number of input tones, output varies. In this chapter, nonlinear distortion is examined for single tone, two tones and multi tones inputs to characterize nonlinear system with simple sinusoidal input(s).

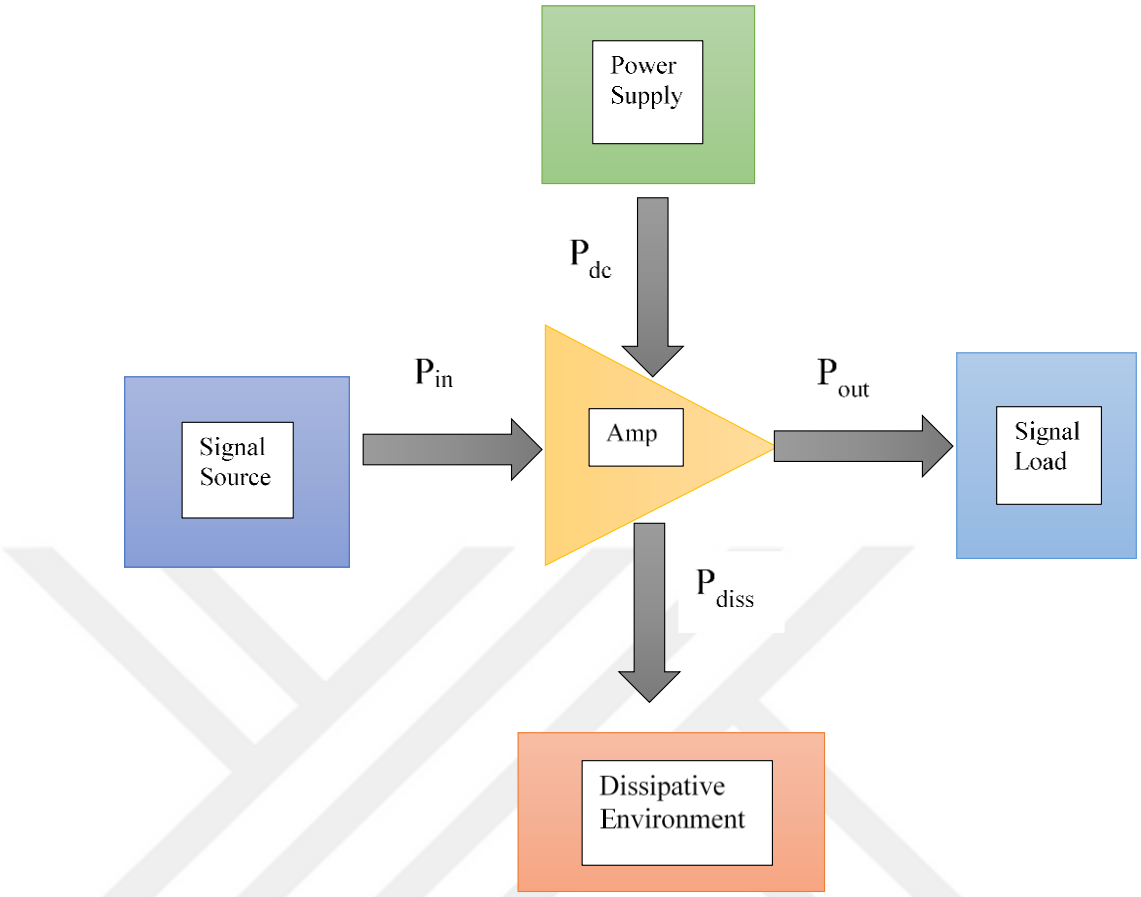

Figure 3.1. Input and output relations of PA

3.2 Single Tone Input

a) Harmonic Distortion

For the communication systems, one tone, which is consist of a simple bandlimited sinusoidal signal, is driven to the system as given in Eq. 3.6.

$$x(t) = A(t)cos[\omega_c t + \theta(t)] \tag{3.6}$$

In memoryless linear time invariant systems, only the amplitude and the phase would be distorted as given in Eq. 3.7.

$$y(t) = a_1 A(t)cos[\omega_c + \theta(t) - \phi] \tag{3.7}$$

However for the memoryless nonlinear time invariant systems, the output is obtained by using Eq. 3.5 and can be written as in Eq. 3.8 up to third order with the assumption that $\theta(t)$ and ϕ_n are equal to zero.

$$y(t) = a_1 A(t)\, cos[\omega_c t] + a_2 A(t)^2 cos[\omega_c t]^2 + a_3 A(t)^3 cos[\omega_c t]^3 \qquad (3.8)$$

By using the trigonometric properties, Eq. 3.8 can be written as Eq. 3.9.

$$y(t) = \frac{a_2 A^2}{2} + \left(a_1 A + \frac{3a_3 A^3}{4}\right)\cos(\omega t) + \frac{a_2 A^2}{2}\cos(2\omega t) + \frac{a_3 A^3}{4}\cos(3\omega t) \qquad (3.9)$$

As seen in Eq. 3.9, three different harmonics occurs at *DC*, $2\omega_c$ and $3\omega_c$ in addition to fundamental frequency ω_c as seen in Figure 3.2. Fortunately harmonics could be rejected by a filtering operation or matching circuit [11].

b) Compression of Output

The factor of fundamental frequency becomes dominant nonlinear distortion component. For small signals, $a_1 A$ is greater than $^{3a_3 A^3}/_4$. However for large signals, the term $^{3a_3 A^3}/_4$ is in the ascendant and while $a_3 < 0$, the output is compressive or saturating. When difference between expected and actual output power equals to 1 dB as seen in Figure 3.3, the system behaves like a nonlinear system. 1 dB compression point has a critical importance for modulation techniques based on envelope fluctuation especially OFDM since it has high PAPR. For peaks above 1 dB compression point are amplified to uncertain values and in demodulation process, this causes errors [11].

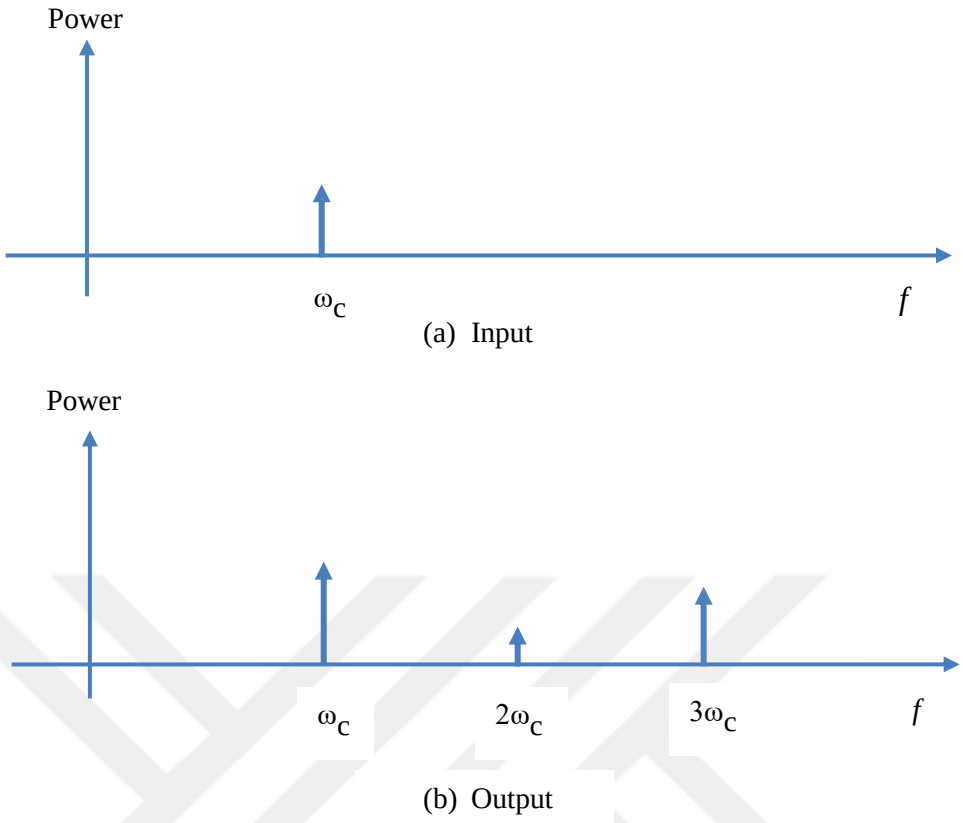

Figure 3.2. (a) One tone input, (b) Fundamental output with harmonics

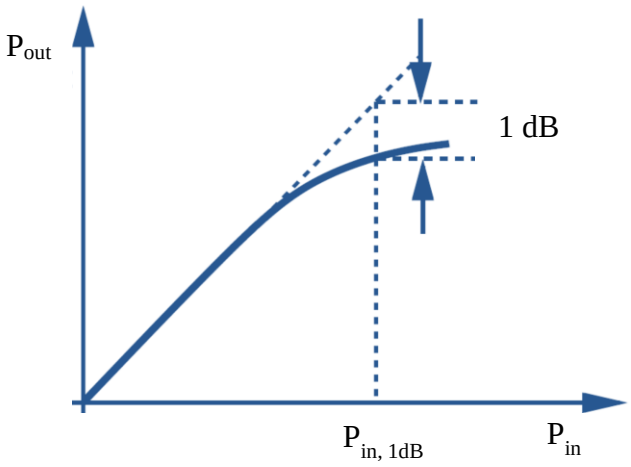

Figure 3.3. 1 dB compression point

3.3 Two Tone Input

Analyzing nonlinear systems with single tone is not adequate. To understand the effects of nonlinearity better, an input signal, which consists of at least two closer frequency bandlimited signals, has to be driven as seen in Figure 3.4 and given as in Eq. 3.10. By inserting these signals to the memoryless time invariant nonlinear system model in Eq. 3.5 up to third order, Eq. 3.11 is obtained. Again, by using trigonometric properties, both in band and out of band components occur in the spectrum as listed the linear components frequencies in Table 3.1 and the harmonic frequencies in Table 3.2. The fundamental components' coefficients are given in Eq. 3.12. These are correlated with the fundamental components and they consist of identical information. However, the rest of them are uncorrelated with the fundamental and they cause noise and spectrum regrowth. Nonlinear distortion effects are discussed below as intermodulation, cross modulation and desensitization.

$$x(t) = A_1 cos(\omega_1 t) + A_2 cos(\omega_2 t)) \tag{3.10}$$

$$\begin{aligned} y(t) = {} & a_1(A_1 cos(\omega_1 t) + A_2 cos(\omega_2 t)) \\ & + a_2(A_1 cos(\omega_1 t) + A_2 cos(\omega_2 t))^2 \\ & + a_3(A_1 cos(\omega_1 t) + A_2 cos(\omega_2 t))^3 \end{aligned} \tag{3.11}$$

$$\begin{aligned} \omega_1 &: \left(a_1 A_1 + \frac{3}{4} a_3 A_1^3 + \frac{3}{2} a_3 A_1 A_2^2\right) cos\omega_1 t \\ \omega_2 &: \left(a_1 A_2 + \frac{3}{4} a_3 A_2^3 + \frac{3}{2} a_3 A_2 A_1^2\right) cos\omega_2 t \end{aligned} \tag{3.12}$$

Table 3.1: Linear Components.

Frequency Component	Type of Response
$-\omega_2$	Linear
$-\omega_1$	Linear
ω_1	Linear
ω_2	Linear

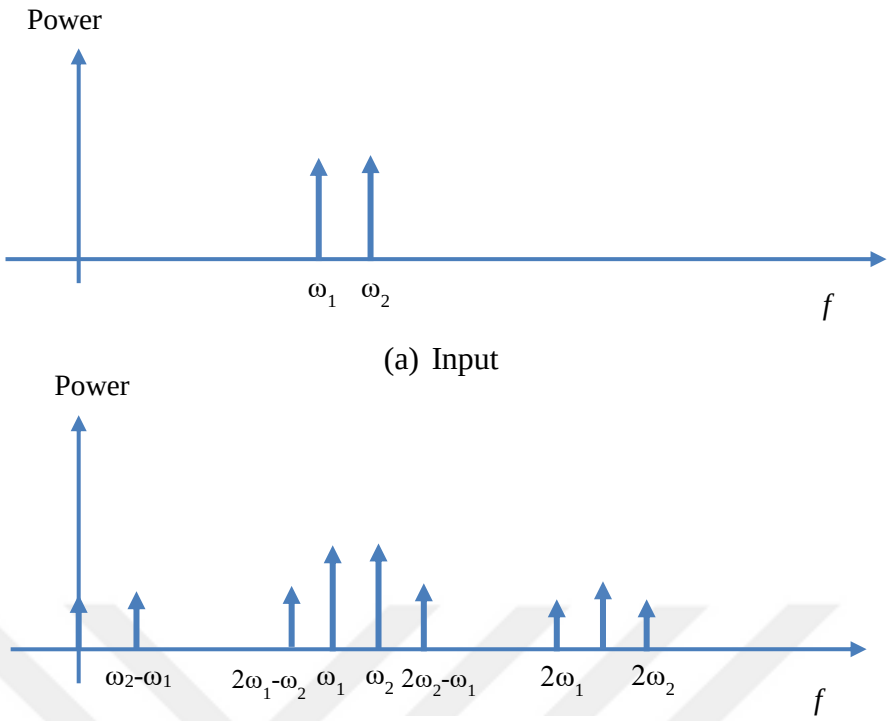

Figure 3.4: (a) Input with two tone signal (b) Output of nonlinear system

Table 3.2: Harmonic Components.

Frequency Component	**Type of Response**
$-2\omega_2$	Second order harmonic distortion
$-2\omega_1$	Second order harmonic distortion
$2\omega_1$	Second order harmonic distortion
$2\omega_2$	Second order harmonic distortion
$-3\omega_2$	Third order harmonic distortion
$-3\omega_1$	Third order harmonic distortion
$3\omega_1$	Third order harmonic distortion
$3\omega_2$	Third order harmonic distortion
0	Shift of bias point
0	Shift of bias point

a) Intermodulation Distortion

For single tone input, new components with the frequencies 2ω, 3ω, 4ω, etc. which are called harmonics are demonstrated previously. However as seen in Table 3.3, when two tones are applied to nonlinear systems, newer components exhibit in spectrum with different frequencies, additional to fundamental and harmonics frequencies. These are called intermodulation distortion (IMD) components. In Eq. 3.13, lower and upper intermodulation components are given. In this equation, $\omega_1 + \omega_2$, $2\omega_1 + \omega_2$ and $2\omega_2 + \omega_1$ are second and third order out of band components and could be rejected by using filtering operation or matching circuit. However, the components at the frequencies $2\omega_1 - \omega_2$ and $2\omega_2 - \omega_1$ are very close to fundamental frequencies and called third order in band intermodulation components. Furthermore, for fifth order $3\omega_1 - 2\omega_2$ and $3\omega_2 - 2\omega_1$ and for seventh order $4\omega_1 - 3\omega_2$ and $4\omega_2 - 3\omega_1$ as given in Figure 3.5 and so not only increase co-channel interference by defining new components but also increase ACI.

$$\begin{aligned} \omega = \omega_1 \pm \omega_2 : & \; a_2 A_1 A_2 \cos((\omega_1 + \omega_2)t) \\ & + \; a_2 A_1 A_2 \cos((\omega_1 - \omega_2)t) \\ 2\omega_1 \pm \omega_2 : & \; \frac{3a_3 A_1^2 A_2}{4} \cos((2\omega_1 + \omega_2)t) \\ & + \frac{3a_3 A_1^2 A_2}{4} \cos((2\omega_1 - \omega_2)t) \\ 2\omega_2 \pm \omega_1 : & \; \frac{3a_3 A_2^2 A_1}{4} cos((2\omega_2 + \omega_1)t) \\ & + \frac{3a_3 A_2^2 A_1}{4} cos((2\omega_2 - \omega_1)t) \end{aligned} \qquad (3.13)$$

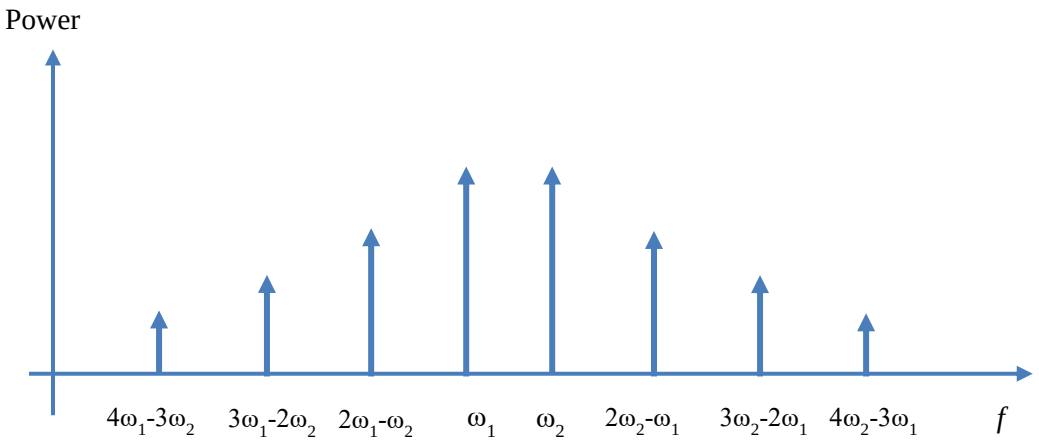

Figure 3.5. Intermodulation distortion components

From Eq. 3.12, fundamental frequency component coefficient is $a_1 A$ and third order intermodulation component coefficient is $(3/4)\, a_3 A^3$ as given in Eq. 3.13 for equal amplitude input signals. While A increases third order intermodulation component increases more quickly than the fundamental component. In Figure 3.6, third intercept point (IP3) which informs about intermodulation behavior of nonlinear system, is illustrated when the fundamental and intermodulation components are equal.

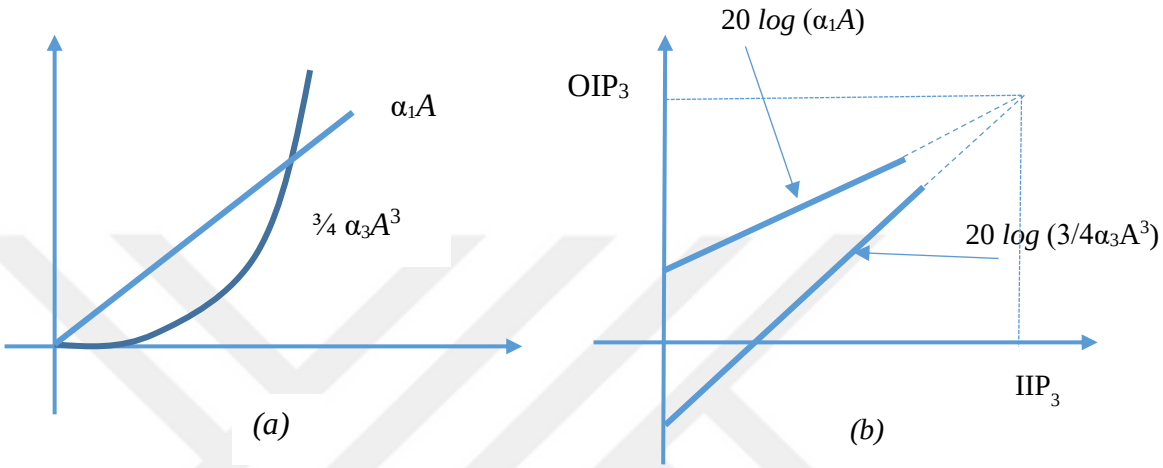

Figure 3.6. Third order intercept point

Table 3.3: Intermodulation Components.

Frequency Component	Type of Response
$-\omega_1 - \omega_2$	Second order intermodulation distortion
$\omega_1 - \omega_2$	Second order intermodulation distortion
$\omega_2 - \omega_1$	Second order intermodulation distortion
$\omega_1 + \omega_2$	Second order intermodulation distortion
$-2\omega_2 - \omega_1$	Third Order Intermodulation Distortion
$-2\omega_1 - \omega_2$	Third Order Intermodulation Distortion
$-2\omega_2 + \omega_1$	Third Order Intermodulation Distortion
$-2\omega_1 + \omega_2$	Third Order Intermodulation Distortion
$2\omega_1 - \omega_2$	Third Order Intermodulation Distortion
$2\omega_2 - \omega_1$	Third Order Intermodulation Distortion
$2\omega_1 + \omega_2$	Third Order Intermodulation Distortion
$2\omega_2 + \omega_1$	Third Order Intermodulation Distortion

b) Cross Modulation

Communications channels are closely separated. Fundamental frequency components' coefficients which are given in Eq. 3.12, are factor to each other as seen in Eq. 3.14.

$$\frac{3}{2}a_3{A_1}^2A_2\cos(\omega_2 t) \qquad (3.14)$$

In this equation, the effect of the tone at ω_1 onto ω_2 is seen and it happens vise versa. However when the tone at ω_1 is modulated with an amplitude modulation technique, envelope will be depended on time and Eq. 3.14 becomes as Eq. 3.15.

$$\frac{3}{2}a_3A_1(t)^2A_2\cos(\omega_2 t) \qquad (3.15)$$

As seen in Eq. 3.15, the tone at ω_1 modulates the tone at ω_2 as illustrated in Figure 3.7. This phenomenon is known as cross talk between channels. In multicarrier systems especially in OFDM system, cross modulation affects system performance adversely. All the components up to third order expansion, which cause cross modulation, are listed in Table 3.4.

Table 3.4: Cross modulation and desensitization Components.

Frequency Component	Type of Response
$-\omega_2$	Cross modulation and desensitization
$-\omega_1$	Cross modulation and desensitization
ω_1	Cross modulation and desensitization
ω_2	Cross modulation and desensitization

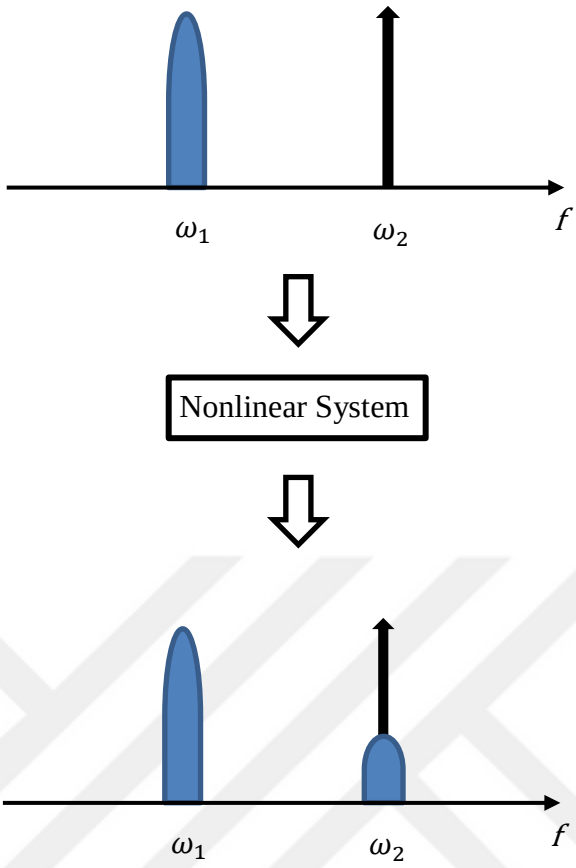

Figure 3.7. Cross modulation

c) Desensitization

Power of input tones in nonlinear systems may vary. In some cases power of the component at ω_1 is much greater than the power at ω_2. According to Eq. 3.12, the coefficient of the component at ω_1 is $a_1A_2 + \frac{3}{4}a_3A_2^3 + \frac{3}{2}a_3A_2A_1^2$. While $A_1 \gg A_2$, ascendant term becomes A_1. The gain of the component at ω_2 is compressed and controlled with ω_1. Especially in OFDM systems, subcarrier with higher peak power desensitizes subcarriers with lower peak powers and degrades system performance. All the components up to third order expansion, which cause desensitization modulation, are listed in Table 3.4.

3.4 Multitone Input

Previously with two tone test, it is seen that nonlinear systems exhibit several new components in the spectrum. Some of them occur in the out of band and could be neglected because they can be removed easily. However rest of them fall into concerned band and even some of them have the same frequency as the fundamental ones. These components decrease efficiency of the system by defining intermodulation distortion, cross modulation, desensitization, etc.

Today's communication techniques consist of multiple carriers particularly OFDM systems. A simple OFDM symbol consists of 64 orthogonal subcarriers and with the guard interval this number could be increased 80 or more. When we evaluate Eq. 3.5 for those subcarriers, excessive number of components would be obtained even for third order. Researcher proposed techniques [57-60] to extract IMD components. Furthermore researcher are proposed methods [61-63] to model memoryless nonlinear system. However some of them are complicated and some of them are not reliable. And also the models are dependent on the input types i.e. whether they are correlated or uncorrelated.

Nonlinearity of a system can be measured by common techniques in two ways. The first one is Noise Power Ratio (NPR) which is based on removing fundamentals and feeding the system with sliced input by using a narrow notch filter as seen in Figure 3.8. The ratio between noise in the notch and output power gives NPR as seen in Eq. 3.16.

$$NPR(\omega_T) = \frac{S_o(\omega_T)}{S_{wd}(\omega_T)} \tag{3.16}$$

The second way to measure nonlinearity is the ratio of the main channel power, P_o with adjacent channel power which is measured with a distance with an offset from the center frequency P_L and P_U as given in Eq. 3.17 and as seen Figure 3.9.

$$ACPR = \frac{P_{L/U}}{P_O} \tag{3.17}$$

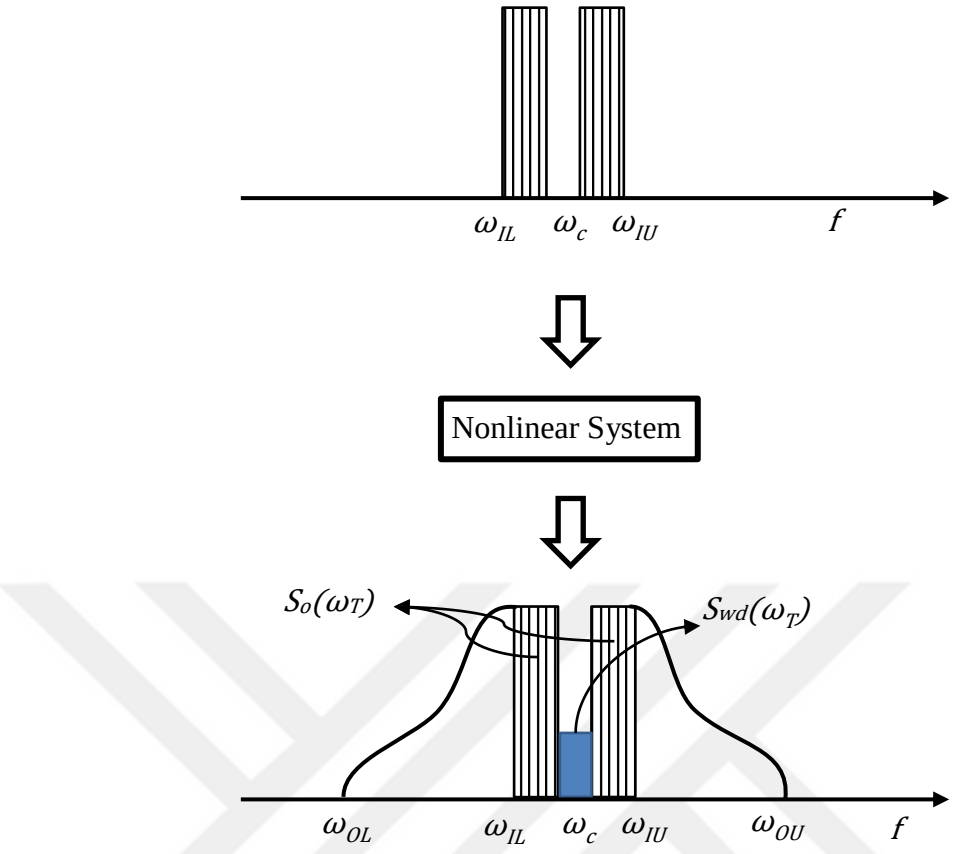

Figure 3.8. Noise power ratio measurement

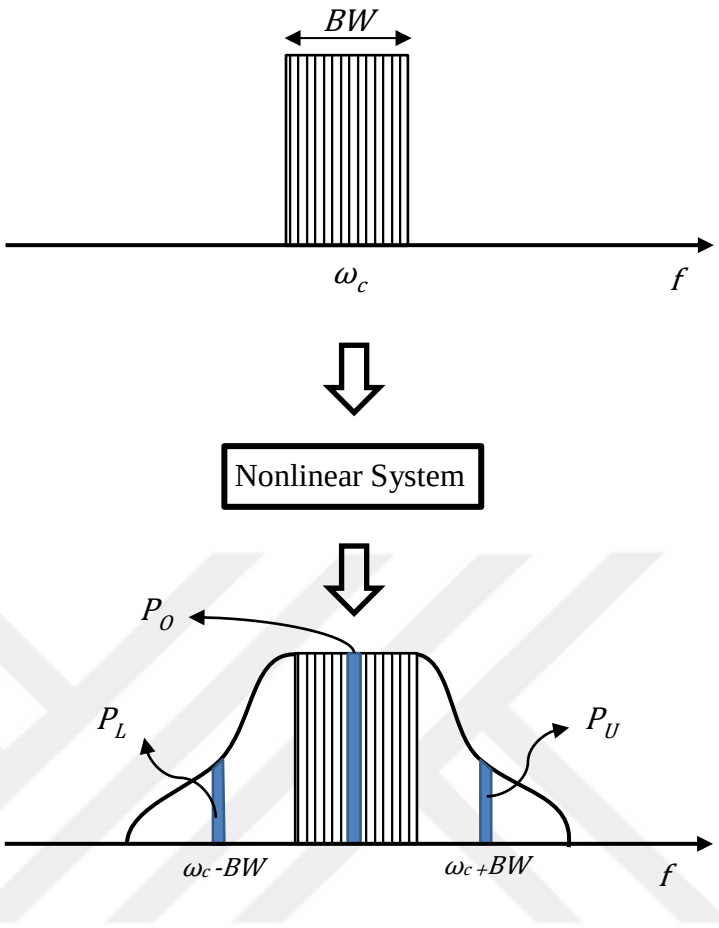

Figure 3.9. ACPR measurement

CHAPTER 4

PAPR REDUCTION WITH TONE INJECTION

4.1 Introduction

In the previous chapters, OFDM system's advantages and disadvantages are described. As given in Chapter 2, OFDM system could be affected by distortions because of its high envelope fluctuation. In Chapter 3, distortion sources are given briefly and it is seen that, effects of nonlinear distortion components are not easily observable especially for multitoned inputs. Unfortunately, these components affect OFDM system performance negatively in addition to increasing adjacent channel interference. PAPR reduction is an efficient way to decrease nonlinear distortion and several techniques have been proposed to achieve the reduction. In Section 2, brief information about PAPR reduction techniques are given and in Section 3, Tone Injection (TI) is explain in detail. In this thesis, SA algorithm is proposed to use with TI technique as the optimization method. In Section 4, Simulate Annealing (SA) algorithm is described in detail.

4.2 PAPR Reduction Techniques

In order to decrease nonlinear distortion in communication systems, several PAPR reduction techniques have been proposed such as Clipping [19,20], Nonlinear Companding Transform (NCT) [21,22], Tone Reservation (TR) [23,24], Partial Transmission Sequence (PTS) [32-38], Selective Mapping (SLM) [39,40],

Constellation Extension [41,42], etc. These techniques can be classified mainly into two groups according to input and output signal relations, with distortion and without distortion.

Clipping is the preliminary version of PAPR reduction technique. The idea is to clip peaks greater than threshold, *A*, as seen in Eq. 4.1[19,20].

$$C_{clip}(x) = \begin{cases} x, & x \leq A \\ A, & x > A \end{cases} \qquad (4.1)$$

However, clipping peaks introduce in band and out of band distortion components. As seen in Figure 4.1 when the clipping factor is equals to 1.2, clipping technique lead to 15 dBc ACPR increase at frequency 1 MHz from the carrier. Receiver is not able to estimate clipped signals correctly, and this causes an increase in BER despite of an influence in nonlinear distortion. Out of band components can be rejected by filtering unfortunately this process also distorts the signal.

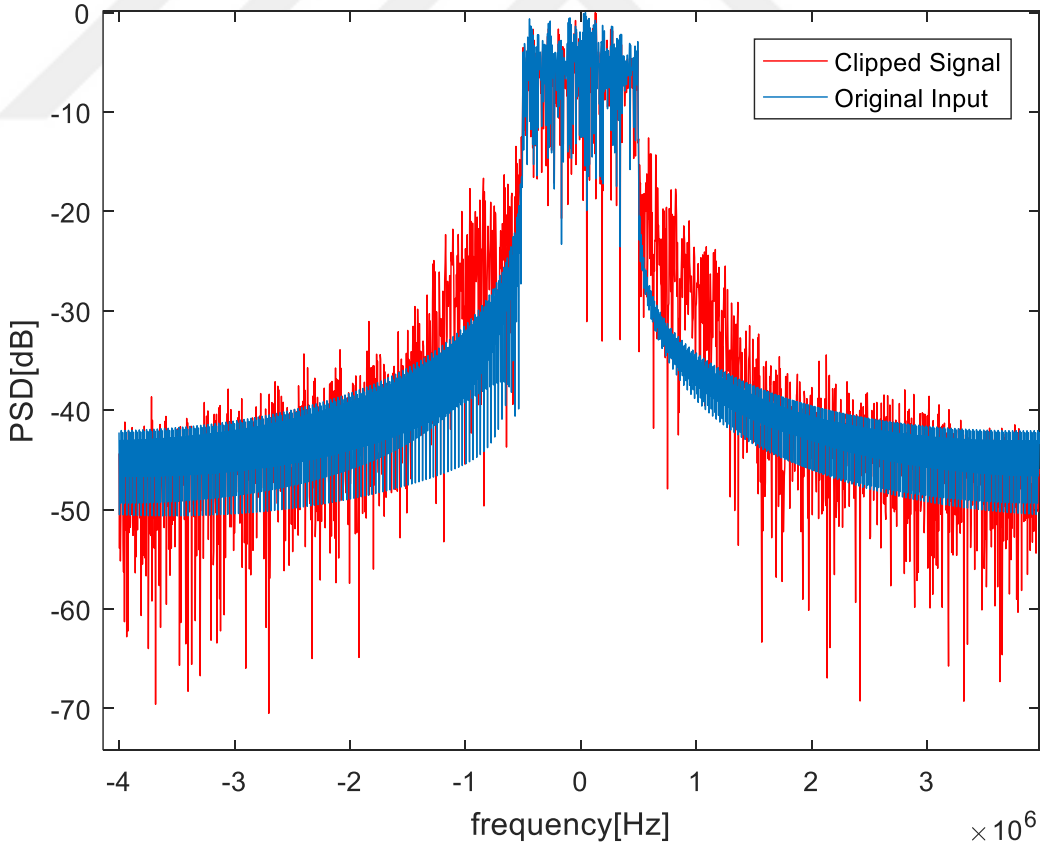

Figure 4.1. Clipping effect on OFDM signal

NTC technique has similar approach to Clipping however in NTC, small signals are enlarged up to peaks levels, and so increasing average power decreases PAPR [21,22]. As similar to Clipping, using NTC technique also introduces in band and out of band components due to companding noise.

TR technique does not distort signal, and part of subcarriers are reserved to be used in the PAPR reduction as seen in Figure 4.2 [23,24]. Position and content of reserved subcarriers are decided iteratively and these are sent to receiver as side information. TR technique provides reduction in PAPR however because of both side information and absent subcarriers, the technique reduces transformation rate.

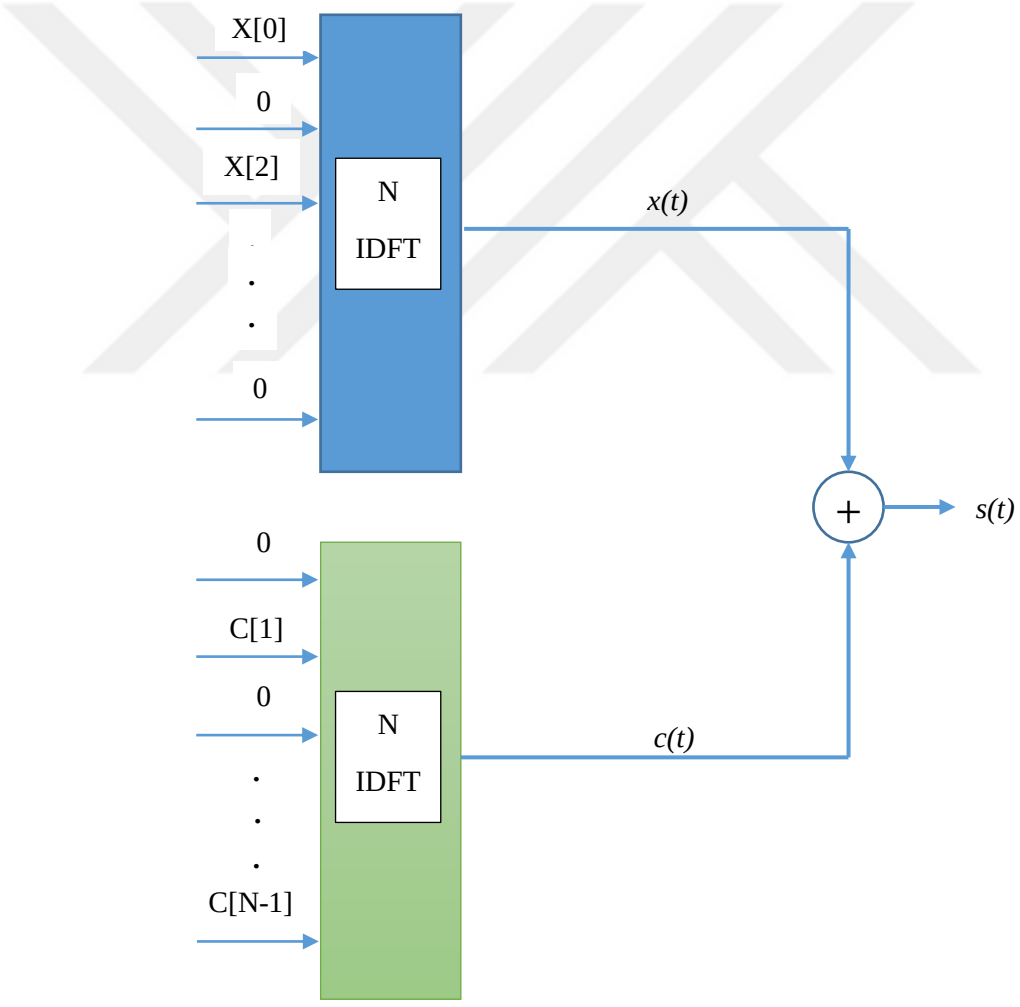

Figure 4.2. Tone reservation schematic

In SLM technique, frequency domain components, i.e. the signal before IFFT operation is multiplied by a phase vector b_v to reduce PAPR as given in Eq. 4.2 [39,40].

$$\check{x}[n] = \frac{1}{\sqrt{N}} \sum_{k=0}^{N-1} X_k b_v e^{j2\pi kn/N} \quad n = 0, .., N \tag{4.2}$$

In PTS technique, time domain components are multiplied by a phase vector as given in Eq. 4.3 [21-27].

$$\check{x}[n] = b_v . x[n] \tag{4.3}$$

Both in SLM and PST techniques, decision of phase vector is a complex process and also the vector has to be sent to receiver with the side information so that the original signal will be recovered.

4.3 Tone Injection

Envelope of OFDM symbol, which compromises of subcarriers, takes form in the IDFT block. Subcarriers are formed by Eq. 4.4

$$\begin{bmatrix} x_0 \\ \vdots \\ x_{N-1} \end{bmatrix}_{Nx1} = Q_{NxN} \begin{bmatrix} X_0 \\ \vdots \\ X_{N-1} \end{bmatrix}_{Nx1} \tag{4.4}$$

where Q is the IDFT matrix with size of NxN, X_n is QAM modulated data and x_n is the n^{th} subcarrier. As seen in Eq. 4.4, each subcarrier is obtained by addition of input sequence by multiplying with different magnitudes. Not only the magnitudes and phases of QAM modulated data components but also the order of the components affects the output of the IDFT.

As previously depicted, PAPR inform about the OFDM symbol and reduction techniques are used to reduce nonlinear distortion of the system. Reordering or changing the QAM modulated signals may decrease the peaks or create another peak in different location. Tellado and Cioffi introduced TI to decrease PAPR of OFDM

symbol by replacing some of the tones' magnitude and phase [24]. To do this, they introduce new tones in the constellation map by shifting original constellation of original constellation of QAM or QPSK as seen in Figure 4.3. Each symbol may be represented by additional 8 new symbols. By using an optimization algorithm, required number of tones are changed by newer ones to decrease the PAPR of the OFDM symbol.

TI technique could be formulated by using Eq. 4.5.

$$\overline{x}\left[\frac{n}{L}\right] = \frac{1}{\sqrt{N}} \sum_{k=0}^{N-1} (X_k + C_k) e^{j2\pi kn/NL} \tag{4.5}$$

C_k is called injected tones and can be described by using Eq. 4.6 and 4.7. D has to be chosen equal or greater than $d\sqrt{M}$ where M is the size of the constellation, and d is the distance between QAM symbols. If D is chosen lower than $\sqrt{M}$, introduced tones overlap with the original constellation and this increases the BER. p_k and q_k parameters are used to decide whether the k^{th} data symbol is to be changed or kept. When p_k and q_k equal to zero, original symbol is used.

$$C_k = Dp_k + jDq_k \tag{4.6}$$

$$\mathrm{p_k}, \mathrm{q_k} \in \{-1, 0, +1\} \tag{4.7}$$

It is obvious that the injected tones increase the average power of OFDM symbol, since they have more energy than original ones. In [64], when the original constellation is moved in only one axis, minimum power increase is calculated by using Eq. 4.8 and it is also depicted that, for some cases power of injected tone may be 30 times more than original tones.

$$\frac{6\sqrt{M}}{N(M-1)} \tag{4.8}$$

From Eq. 4.4, it could be deduced that, when the tones is changed with opposite sign tones, the envelope would be evolved more dramatically. Ohta *et al.* [27] state that,

outer tones with larger amplitude are dominant on signal envelope and changing them with their conjugates results with drastically variations. Also constellation map given in Figure 4.3 cause redundant power increase. So, to limit the power increase they propose a new constellation map in Figure 4.4. As seen in the map, only the outer tones are taken into account and defined new tones for them. Thus with using proposed map not only limits the power increase but also reduces possible combinations. Since when the constellation map in Figure 4.3 is used, each symbol could be changed with 8 different values. However in the new constellation, only the outer tones are changed, and they have only single candidate.

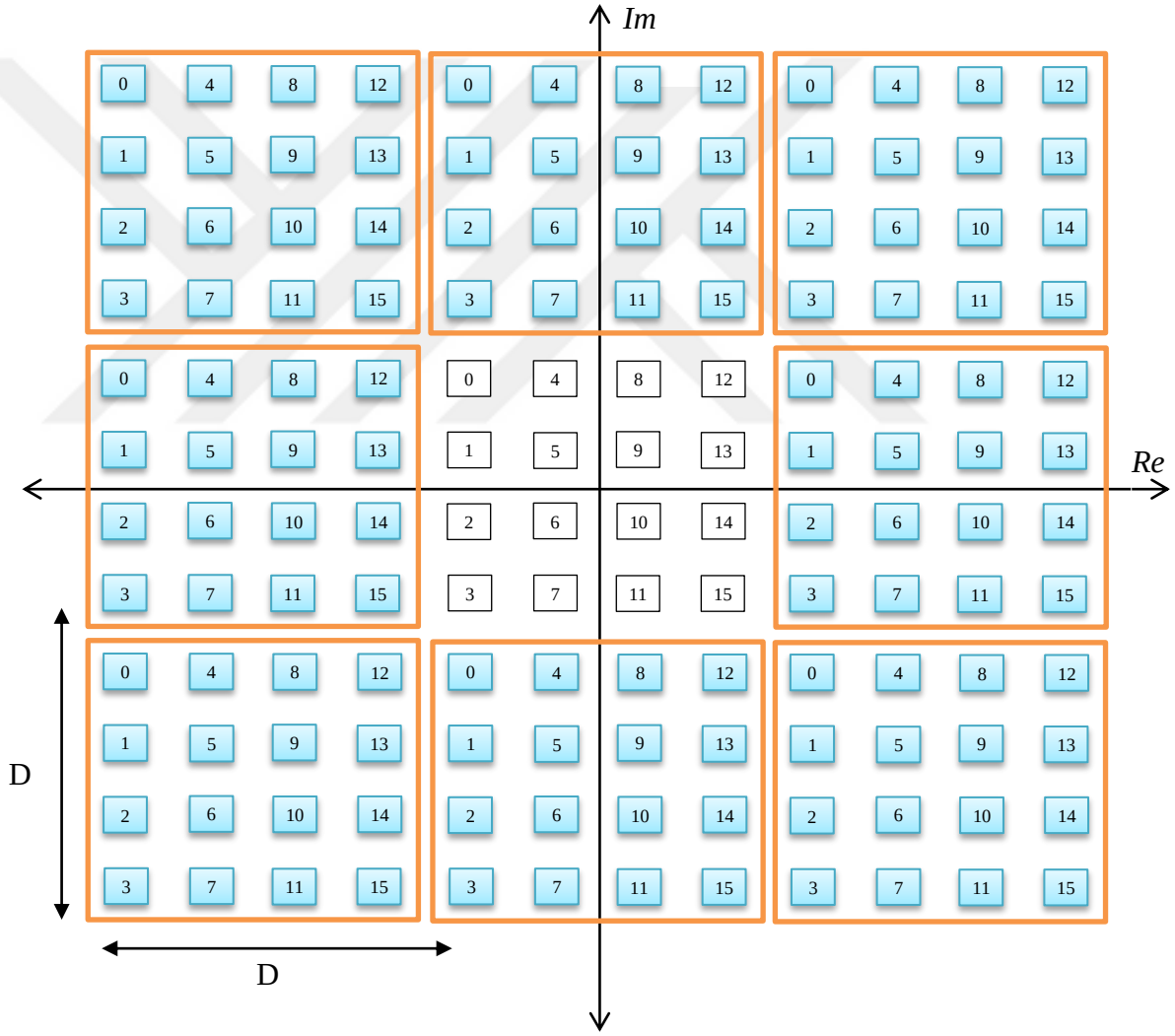

Figure 4.3. Tellado and Cioffi' proposed constellation

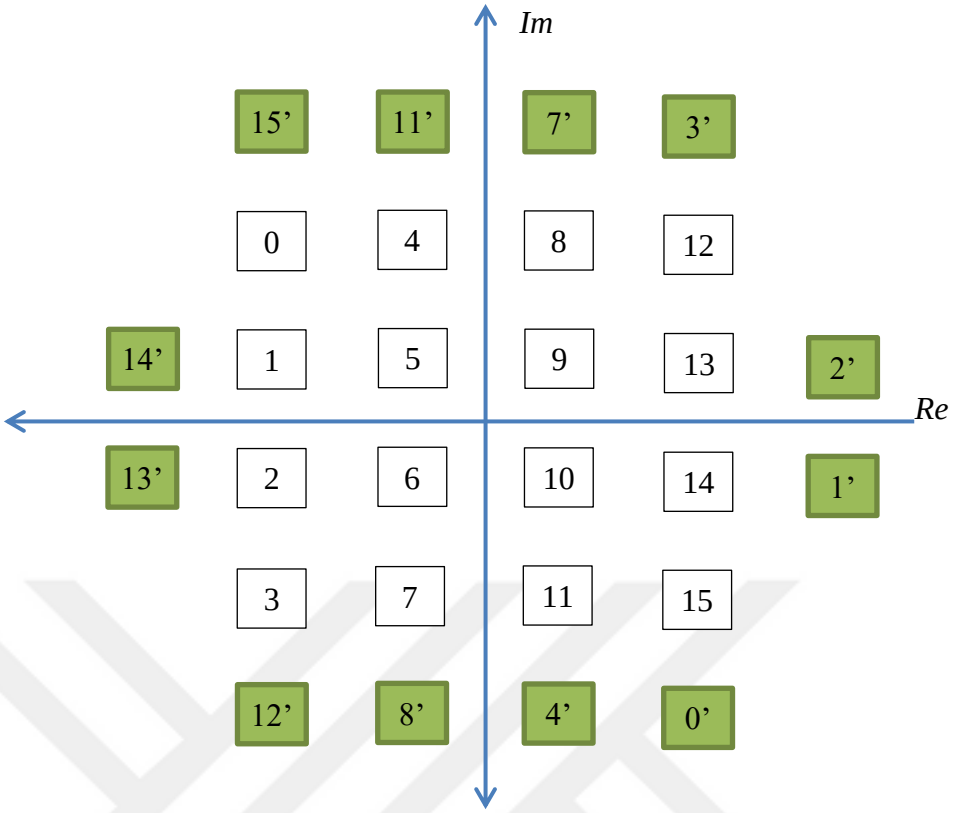

Figure 4.4. Mapper constellation

TI reduces PAPR without data rate loss and without using the side information, and its implementation is easy. In transmitter chain, TI is carried out after IDFT block. For the tones higher than the threshold, it injects appropriate tones. In the receiver chain, injected tones are detected by reorganized demapper according to extended constellation as seen in Figure 4.5.

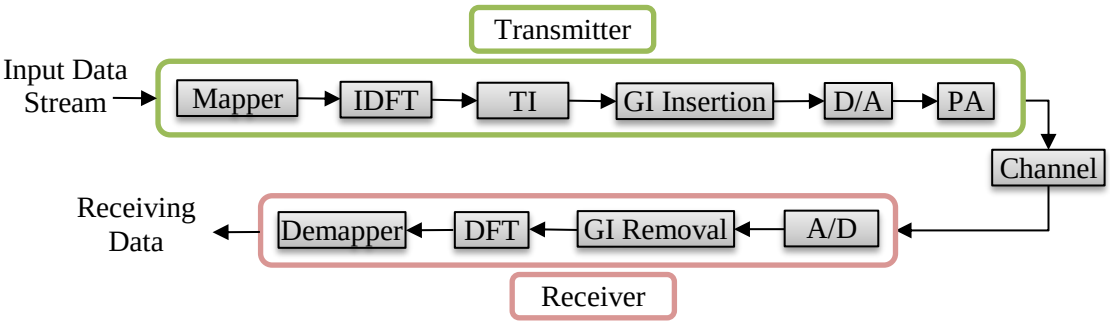

Figure 4.5. Transmitter and receiver architecture with TI technique

Tones in OFDM symbol can be changed directly with the new ones. However, this does not guarantee reduction on PAPR. Moreover, it increases the average power and may create larger ones. Studies show that changing limited number of tones also decreases PAPR. Considering large number of subcarriers and all the combinations, TI becomes challenging and time consuming process and PAPR reduction becomes combinatorial optimization problem.

Heuristic approaches are used in solving these problems and the approaches usually take a considerable time to reach a solution. They aim to reduce computation time, rather than to provide an accurate solution. Researchers use Greedy algorithm [24], linear programming [25], parallel stochastic search [26], neural networks [27], genetic algorithm [28], tabu search [29], cross entropy [30] and aggressive clipping [31] methods in literature. Optimizations based on searching in created data set complicates the operation [26,28,29], since several combinations have to be considered to create data set and for each combination an IFFT operation has to be carried out. These data have to be stored on embedded systems, which will allocate resources. To decrease the IFFT size, researchers apply windowing operation to the envelope. As previously depicted, this process may decrease peak in focus window, however it may also create another peak.

4.4 Simulated Annealing (SA)

SA, which is introduced by Kirkpatrick, Gelatt, and Vecchi [43], is used to find global minimum or maximum of a cost function through probabilistic approach. The process imitates cooling of materials by time i.e. in the algorithm, a parameter called temperature (T) is decreased by time. Algorithm searches in wider solution space for higher T, and while T is decreased, algorithm searches a possible solution in narrow space.

SA algorithm can be used with PAPR reduction algorithms and these algorithms need to carry out an IDFT operation in each iteration. In Figure 4.6, flowchart of SA algorithm is given. In SA method, energy of the system or in other words value of the function is calculated by objective function $E(x_i)$, in this case its PAPR value, at the state x_i. The next state x_{i+1} is determined randomly and the energy change, ΔE, is calculated using Eq. 4.9.

$$\Delta E = E(x_{i+1}) - E(x_i) \tag{4.9}$$

The acceptance of new state is decided by using Metropolis criteria as given in Eq. 4.10.

$$P = \begin{cases} 1, & \Delta E < 0 \\ e^{-\Delta E/T_i} > R, & \Delta E \geq 0 \end{cases} \tag{4.10}$$

T_i is the state temperature and equal to $\alpha \times T_{i-1}$. R is randomly generated number in the interval [0 1]. α is the cooling factor and sets the quickness of cooling. In the higher temperatures, worse trades may be accepted to cover all possible solution space. Algorithm compares the possible solutions and avoid trapping in local minimums. While the temperature is reduced, algorithm searches in confined space to obtain optimum solution.

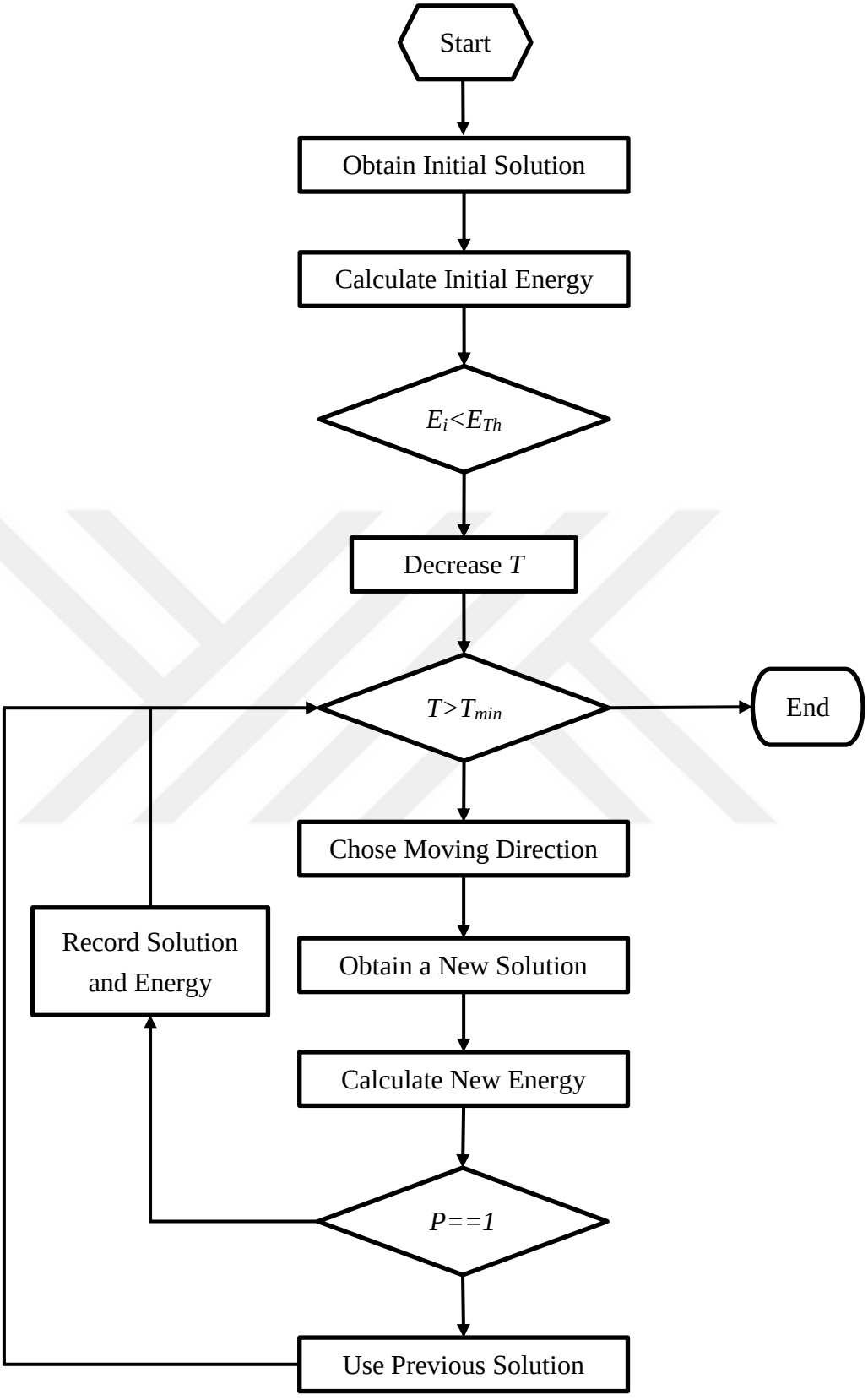

Figure 4.6. Flowchart of SA

CHAPTER 5

SOFTWARE DEFINED RADIO

5.1 Introduction

Today, communication systems are used in different areas, with new functions and new standards. Not only mobile phones and computers but also televisions, cars, watches, refrigerator, etc. are designed to support multiple protocols and standard for voice, video and data communications. In conventional radio design such as Velcro approach, a radio unit has to be developed for each functions. Physical layer functions, which are digital signal processing, analog-digital conversion, RF front end and antennas, are needed to develop separately for each radio.

To bring a new perspective to communication system design, Mitola proposed Software Defined Radio (SDR) concept to use the same hardware with different functions [68]. Digital signal processing, analog-digital conversion, RF front end and antennas can be used for different functions or new functions or standards may be added to SDR platform by reprogramming property of digital signal processor. In Figure 5.1, a basic SDR architecture, which consists of a digital signal processor, RF board (or front end) and amplifier, is given.

By using SDRs, digital communication techniques, which serve different purposes, can be carried out at the same time. Cognitive radio properties can be added to SDR systems.

SDR concept has been used for several years and various SDR definitions were proposed. Among these, commonly used one is “Radio in which some or all of the physical layer functions are software defined”. This definition is given in Wireless Innovation Forum [44]. Most of the devices we used in our daily life can be classified as SDR, such as computers, mobile phones, televisions, etc according this definition. However, some of them do not have reprogrammable digital signal generators and some of them is not produced with wideband RF front end and antennas. In research and development studies, SDR platforms need reprogrammable and multifunctional digital signal processors to apply newer techniques and enhance system performances. Also, they need to have wideband controllable RF front ends and antennas.

In this chapter, basic components of the SDR, signal processor and RF board are described in Section 2 and 3, respectively. In Section 4, programming tools are discussed.

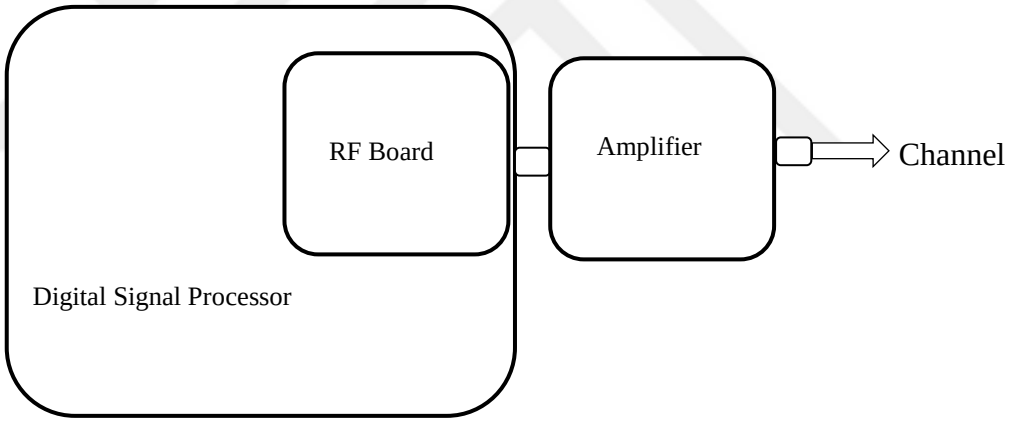

Figure 5.1. Basic SDR architecture

5.2 Signal Processor

As a signal processor, General Propose Processors (GPP), Digital Signal Processors (DSP) and Field Programmable Gate Arrays (FPGA) can be used. GPP and DSP are optimized to perform complex operations with powerful single processor. FPGA is composed of multipliers, memory blocks, AND, OR, NOT, XOR, etc. and these can

be connected one to another according to requirements and multiple different sets can be obtained. These sets may perform different tasks at the same time. Especially for the algorithms, these include operation like DFT which requires parallel processing. FPGA's performance is better than DSP's and GPP's performance. In Figure 5.2, differences of DSP and FPGA are illustrated.

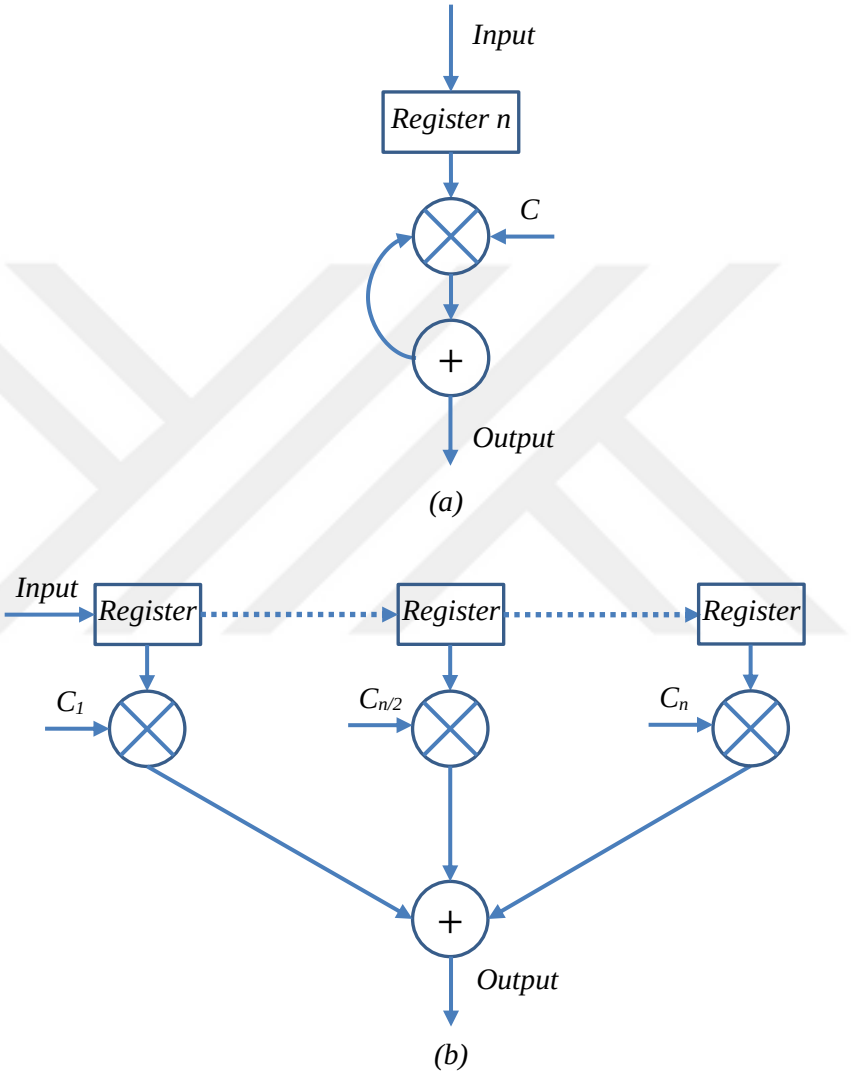

Figure 5.2. Architectures of (a) DSP and (b) FPGA

In the market, several FPGA vendors and various products exist. These products have differed logic cell, block ram, I/O, etc. numbers. However, instead of numbers, development platforms and FMC's are more important for development projects.

Xilinx Virtex 6 EB [65], which has 512 Mb DDR3 SODIMM memory, an 8-lane PCI Express interface, general purpose I/O, high-speed VITA-57 FMC connector, and a UART, is adequate to develop communication system application such as OFDM with PAPR reduction technique.

5.3 RF Board

RF board plays critical role in the SDR as in other commination systems. Transmitter output of the signal processor is digital. RF boards are used to convert the digital signals to analog signals with appropriate sample rate and they modulate the signals with quadrature modulator to the desired frequency and bandwidth. Modulated signal is driven to an amplifier and then it is driven to channel with appropriate method. In the receiver part of the SDR, received analog signal is firstly demodulated and then amplified by using a LNA. Amplified signal is sent to the signal processor after the signal is converted to digital signal by using DAC.

According to the usage area, a wide variety of RF board types exists in the market. However, the RF board has to be in accord with the signal processor and it has to be controllable and programmable. In this manner, Analog Device FMCOMMS1 high-speed analog module [66] is suitable use with Xilinx Virtex 6 EB to generate a wideband communication signal.

FMCOMMS1 provides the analog front-end for a wide range of FPGA-based direct-conversion transceiver applications. A direct-conversion transceiver, also known as homodyne, synchrodyne, or zero-IF transceiver, is a radio transceiver design that (de)modulates the radio signal using a local oscillator (LO) whose frequency is identical to, or very close to, the carrier frequency of the intended signal. The AD9122 DAC which converts the digital signal to analog signal interpolates the data and applies a frequency translation to the baseband. To translate baseband signal to desired RF output frequency, signal is driven to ADL5375 Quadrature Modulator. This signal is then passed through an image rejection filter to an ADL5602 with +20 dB gain. In the receive direction, the signal demodulated by the direct-conversion ADL5380 Quadrature Demodulator is used to demodulate complex baseband signal. Resulting signals are filtered and then passed to the AD8366 digital variable gain amplifier, Before the analog to digital conversion, to remove nonlinear distortion components a

filtering operation is carried out. The AD9643 digitalizes the input signal. In Figure 5.3, block diagram of FMCOMMS1 is given.

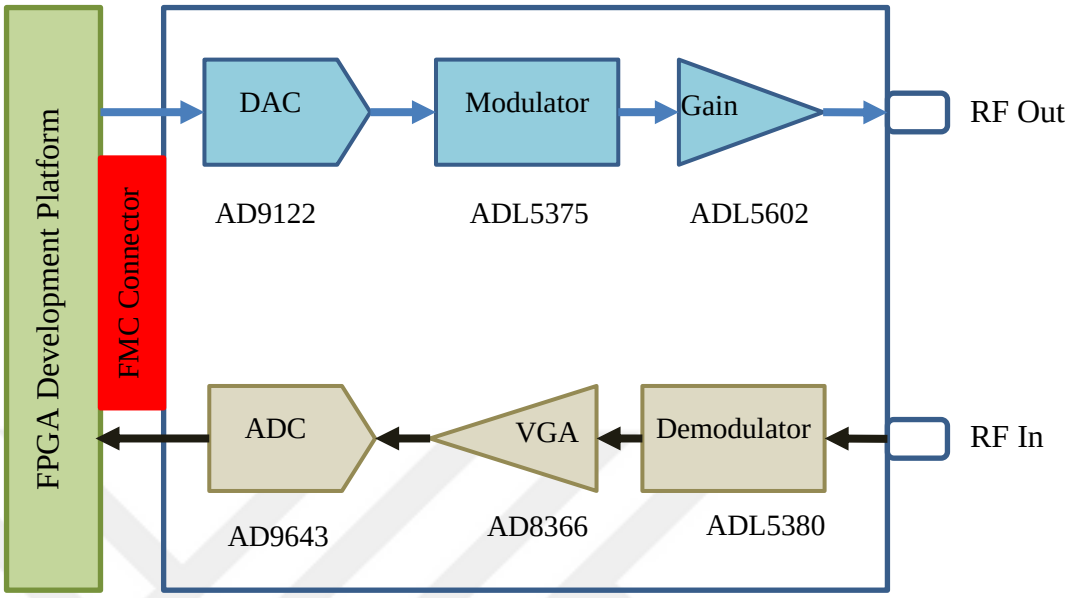

Figure 5.3. Block diagram of FMCOMMS1

5.4 Programming Tools

a) Using ISE with Verilog/VHDL

Verilog and VHDL are Hardware Description Languages (HDL), which are used to program hardware by using the design tools. There are small differences between Verilog and VHDL however, they both perform the same job. Xilinx ISE design suit supports both languages and it can be used in the same design in different modules.

Xilinx provides highly parameterized Intellectual Properties (IP) for Xilinx FPGAs by the CORE Generator. For the communication systems, Xilinx provides the cores such as DDS Compiler, FIR Compiler, FFT, Forward Error Correction IP such as Reed-Solomon Decoder and Encoder, Viterbi Decoder, etc. and these cores can be used during the design process. By using Core Generator, a ChipScope core can be generated to analyze the signals after the implementation level.

Design implementation and verification steps must be carried out from the beginning to the final version of the project. For any changes in the design, these all steps must be repeated and the exact outputs of the device can only be seen after programming.

b) System Generator for DSP

System Generator is a DSP design tool from Xilinx that enables the use of the MathWorks model-based Simulink design environment for FPGA design. By using MATLAB/Simulink, a complete SDR transmitter and receiver model can be developed and simulated. After simulating and verifying the model, Simulink blocks is changed with Xilinx blocks. All the components in the model can be connected easily. System Generator allows to generate bitsteam file using Verilog/VHDL code, File generation is done by using the token and all the necessary clocking signals are generated automatically.

c) MATLAB/Simulink

As it is known, MATLAB and Simulink are used to develop and communication systems with built-in functions and blocks. Developed designs can also be simulated both in time and frequency domains for different channel conditions to provide improvements on system design. MATLAB also allows to design and verify practical communications systems for SDR, which contains FPGA. By the HDL coder, Verilog or VHDL codes of MATLAB functions or blocks can be generated and these codes can be downloaded to the FPGA as a custom bitstream file. By using the HDL optimized Simulink blocks, a system can be modelled and simulated, and then whole system can be prototyped on SDR hardware. The HDL workflow advisor ensures timing requirements and allows resource sharing on hardware for the designed system. Also, the codes can be optimized and the designed SDR performance can be verified after the codes are downloaded to FPGA by using the MATLAB [70].

Most of the functions and blocks of MATLAB are designed to work as frame based. However, user has to design the system as sample based, not as the frame based, and user has to convert the data types double to fixed point by using the Fixed Point tool.

Communication system toolbox supports Xilinx Virtex 6 FPGA EB and Analog Devices AD-FMCOMMS1 FPGA mezzanine cards (FMC). The connection between

FPGA board and FMC card is provided with MATLAB. However, the control on FMC card is limited and some of the card properties are decided by MATLAB.

MATLAB/Simulink also allows the users to send the generated data on PC to the FPGA and RF board. Thereby the data on the PC is converted and upsampled on the FPGA.

CHAPTER 6

RESULTS

6.1 Simulation Results

OFDM systems are used in several communication systems to transmit and receive data. Although the intended use differs, signal generation procedures are the same. In this thesis study, an OFDM system as given in Figure 6.1 is constituted to carry out the simulations and PAPR of OFDM symbol is analyzed and reduced by using TI technique which is performed using SA algorithm as an optimization method.

TI algorithms start with searching the tones on outer ring of the constellation and replace them with new tones in a symbol with high PAPR. Decision of how many tones has to change with new ones is also a critical parameter and affects system performance as far as the optimization algorithm.

In this study, FFT size is chosen as 64 and 48 subchannels of 64 are mapped with the 16-QAM gray code form as seen in Figure 6.2. A DC carrier and guard bands are inserted and PAPR is calculated for randomly generated 10^5 OFDM symbols using Eq. 2.5 with oversampling factor L=4. In SA algorithm, initial temperature and cooling factor are set to 100 and 0.85, respectively. SA algorithm is performed if PAPR is higher than the threshold with 2, 3, 4, 5, and 6 tones to analyze the effect of amount of tone injection on the performance. The algorithm is also run with the inner threshold.

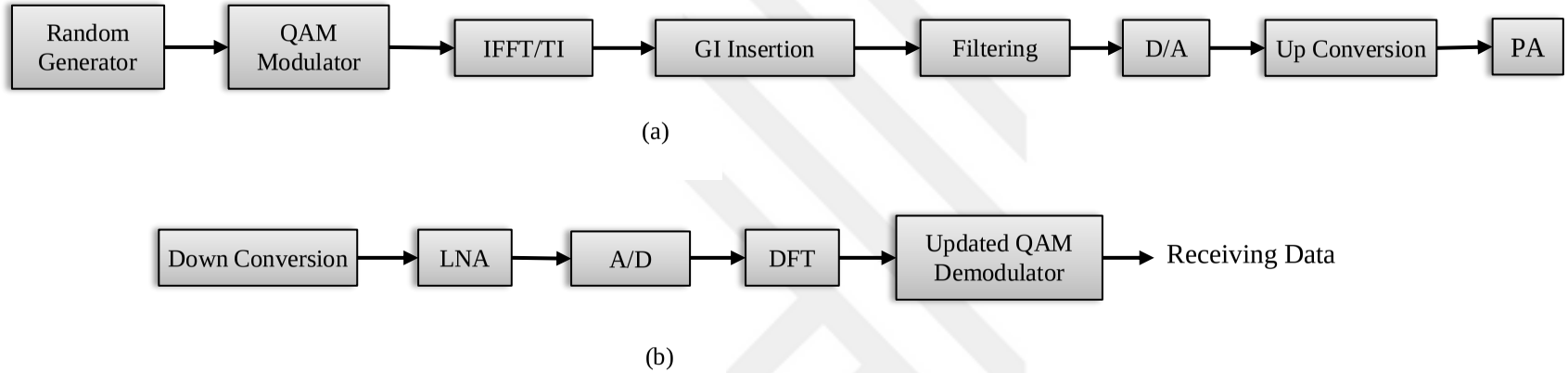

Figure 6.1. a) Transmitter architecture b) Receiver architecture

Optimization stops when a value less than inner threshold is obtained during the iterations.

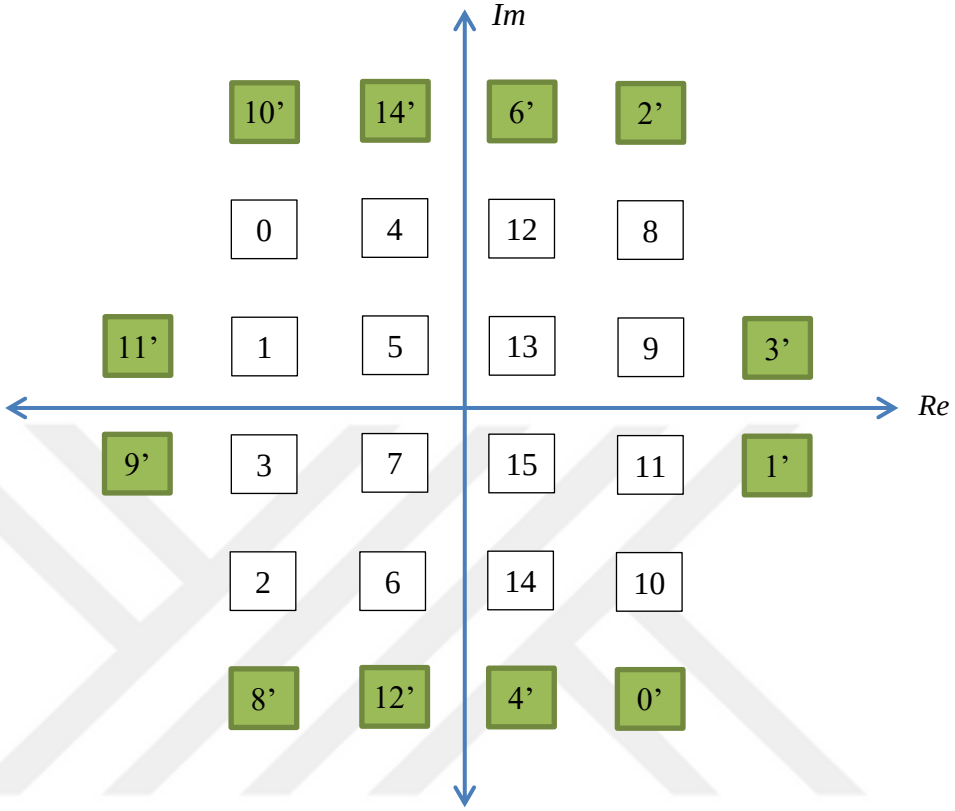

Figure 6.2. Gray code constellation of QAM with injected tones

In Figure 6.3, CCDF of original and reduced PAPRs of 10^5 OFDM symbols are given. As seen in the figure, when Pr[PAPR > PAPR0]=10^{-3}, PAPR of original symbols is 10.4 dB and for 2, 3, 4, 5 and 6 tones injected signals are 7.5, 6, 5.5, 5.5, and 5.4 dB respectively. When the injected tone numbers are chosen as 4, 5 and 6, better results are obtained. Original signals’ PAPR is reduced from 10.5 dB to 5.5. dB and the highest PAPR is equal to 5.5 dB. When 3 tones are injected, highest PAPR is only 0.5 dB above the best results. When two tones are injected, only a 3 dB reduction is obtained. In Table 6.1, the mean of 10^5 OFDM symbols’ average power, peak power, PAPR and iteration numbers are given. As seen in the table, average power of the symbol is increasing proportional to number of tones injected and average of PAPR is reduced to 5.2152, 4.8701, 4.7688, 4.7408, and 4.7283 dB from 7.2728 dB. However,

the necessary iteration numbers to reduce PAPR are obtained usually above 3000. Unfortunately, PAPR reduction techniques are used within a part of OFDM system, which requires high speed data streams. Iteration number such a high is greater than the system can handle.

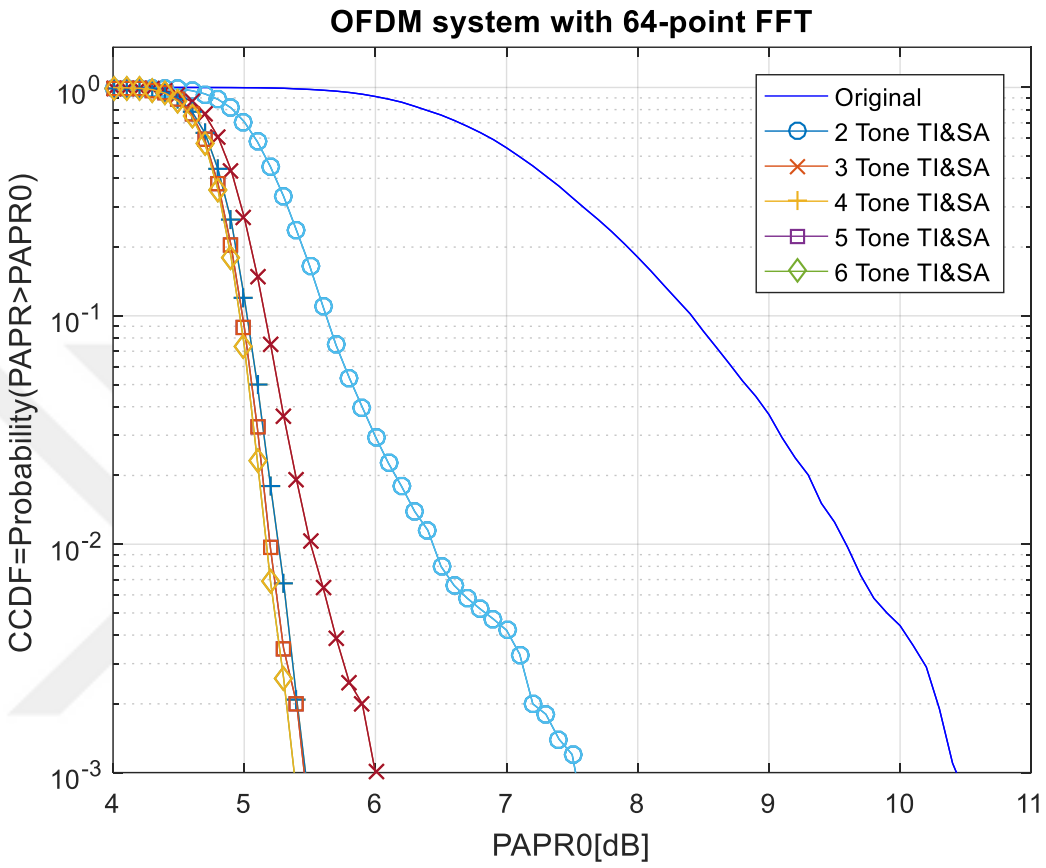

Figure 6.3. PAPR reduction analysis with different number of tones

Table 6.1: PAPR reduction with TI and SA

	Original	**2 tones**	**3 tones**	**4 tones**	**5 tones**	**6 tones**
Average Power (dBW)	-9.30	-9.03	-8.89	-8.76	-8.63	-8.51
Peak Power (dBW)	-2.03	-3.81	-4.02	-3.99	-3.89	-3.79
PAPR (dB)	7.27	5.21	4.87	4.76	4.74	4.72
Number of iterations	-	3696	3456	3423	3432	3419

In Figure 6.4, CCDF of original and reduced PAPRs of 10^5 OFDM symbols' are given when the algorithm runs with 6 dB inner threshold. As seen in the figure, when $Pr[PAPR > PAPR0]=10^{-3}$, PAPR of original symbols is 10.4 dB and apart from the 2

tone injection, PAPR is reduced to 6 dB. In Table 6.2, the mean of 10^5 OFDM symbols' average power, peak power, PAPR and iteration numbers are given for optimization with 6 dB threshold. As seen in the table, average of PAPR is reduced to 5.7591, 5.7222, 5.7154, 5.7125 and 5.7122 dB from 7.2598 dB. In this case, the necessary iteration numbers are dramatically reduced (almost 100 times) considering to PAPR reduction without inner threshold. Especially for 4, 5 and 6 tone injections, 44, 35, and 34 trails are adequate to ensure the inner threshold.

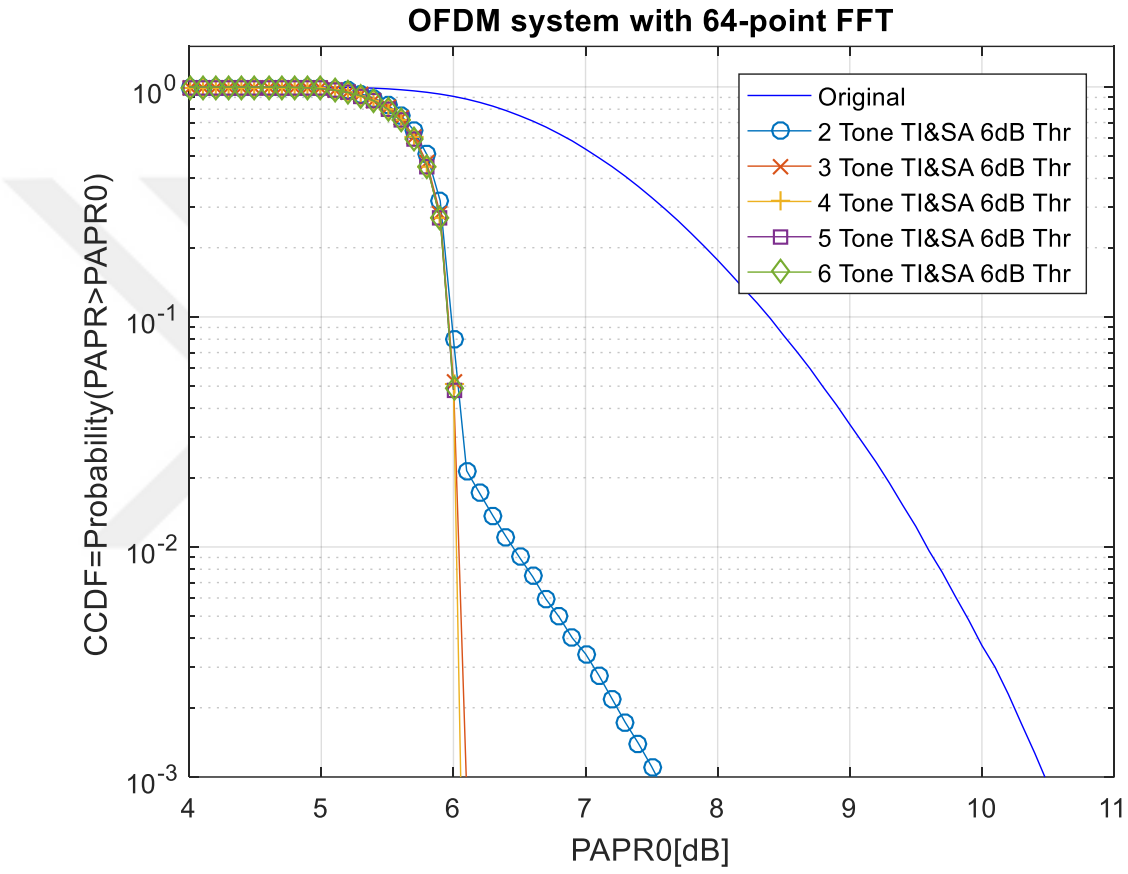

Figure 6.4. PAPR reduction comparison with different number of tones and with 6 dB inner threshold

Table 6.2: TI with SA and with 6 dB threshold.

	Original	2 tones	3 tones	4 tones	5 tones	6 tones
Average Power (dBW)	-9.30	-9.05	-8.93	-8.81	-8.69	-8.58
Peak Power (dBW)	-2.04	-3.29	-3.21	-3.09	-2.98	-2.87
PAPR (dB)	7.25	5.75	5.72	5.71	5.71	5.71
Number of iterations	-	841	112	44	35	34

In Figure 6.5, proposed method in this study is compared with tone injection based linear programing [25], tabu search [29], cross entropy [30], aggressive clipping [31] and joint usage of PST and SA based hybrid of genetic-SA [34] and PST with modified SA [35] PAPR reduction techniques. In Table 6.3, PAPR values is given when $Pr[PAPR>PAPR0]=10^{-3}$. As seen in the graph, when SA algorithm is used with PST technique, only 0.4 dB reduction is obtained. Other methods mentioned above provide a PAPR reduction as nearly 4 dB. It can be observed that the lowest value of PAPR is achieved using the proposed method and the best result is obtained.

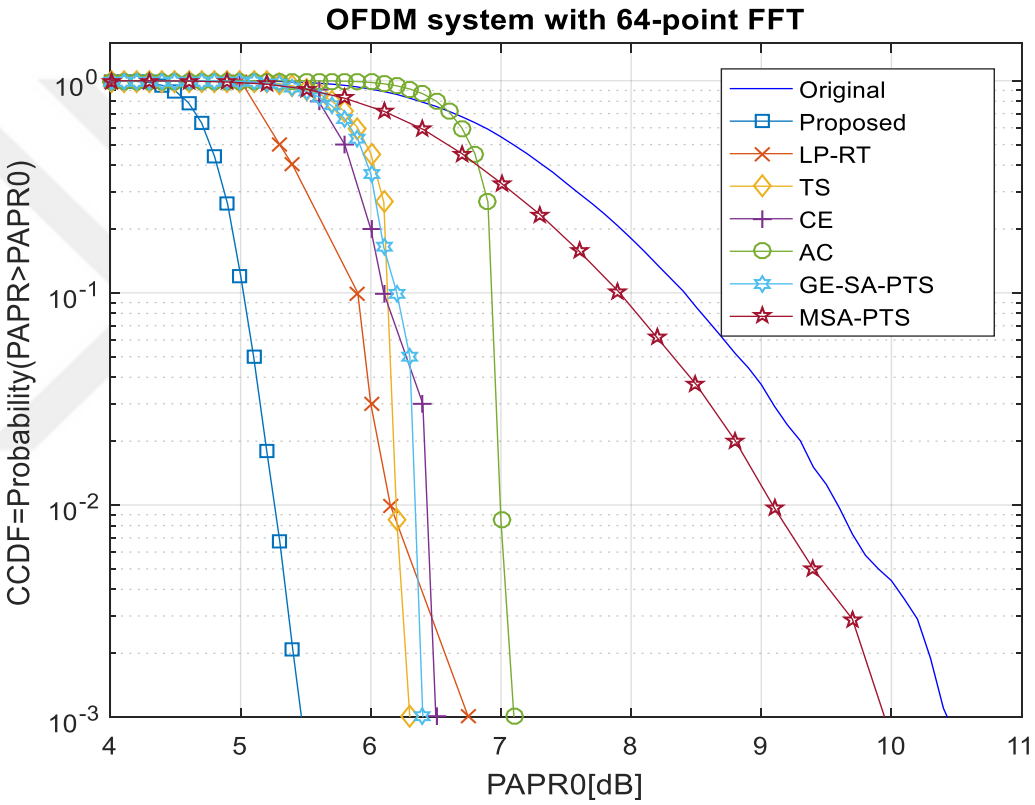

Figure 6.5. Comparison of proposed method and conventional PAPR reduction methods

Table 6.3: Comparison of proposed method with other PAPR reduction techniques.

	Original Signal	Proposed Method	Linear Programing	Tabu Search	Cross Entropy	Aggressive Clipping	Hybrid of Genetic-SA	Modified SA
PAPR (dB)	10.4	5.4	6.75	6.2	6.5	7	6.4	10

Memoryless nonlinearity can be modelled by using Rapp model [62] for the baseband complex signals. To observe and analyze the effect of PAPR reduction in the OFDM symbols, original symbol and PAPR reduced symbol are driven to Rapp model, which adds nonlinear distortion components to the signal without amplification. In Figure 6.6, the input of the model and the outputs of the Rapp model for two symbols carry the same information. As seen in the graph, ACPR of the PAPR reduced symbol is decreased nearly 10 dB according to original symbol at the 1 MHz far from the center frequency. This graph also shows that, PAPR reduction of OFDM symbols results with a reduction in the nonlinear distortion of the system.

6.2 Experimental Results

In this thesis, Xilinx Virtex 6 FPGA ML605 Evaluation Kit [65], ADI FMCOMMS1 Mezzanine Card [66] and RFMD RF5117 Power Amplifier [67] are used together to construct SDR and in Figure 6.7, block diagram of the used SDR platform is given. Together with the SDR system, a 10 dB attenuator is used to protect spectrum analyzer against the high power. In Figure 6.8, Physical appearance of the experiment setup is given.

The OFDM transmitter with TI and SA algorithms, which is described in Section 1, is generated and targeted to the experimental setup. OFDM signal is created on FPGA from input data stream. Each OFDM symbol consists of 64 subcarrier and 48 of the carry data and the rest of them are assigned as virtual carrier. The randomly generated input data stream provided by a desktop computer. The bandwidth of the symbol is set to 1 MHz. PAPR reduction algorithm steps in when PAPR exceeds the predefined threshold.

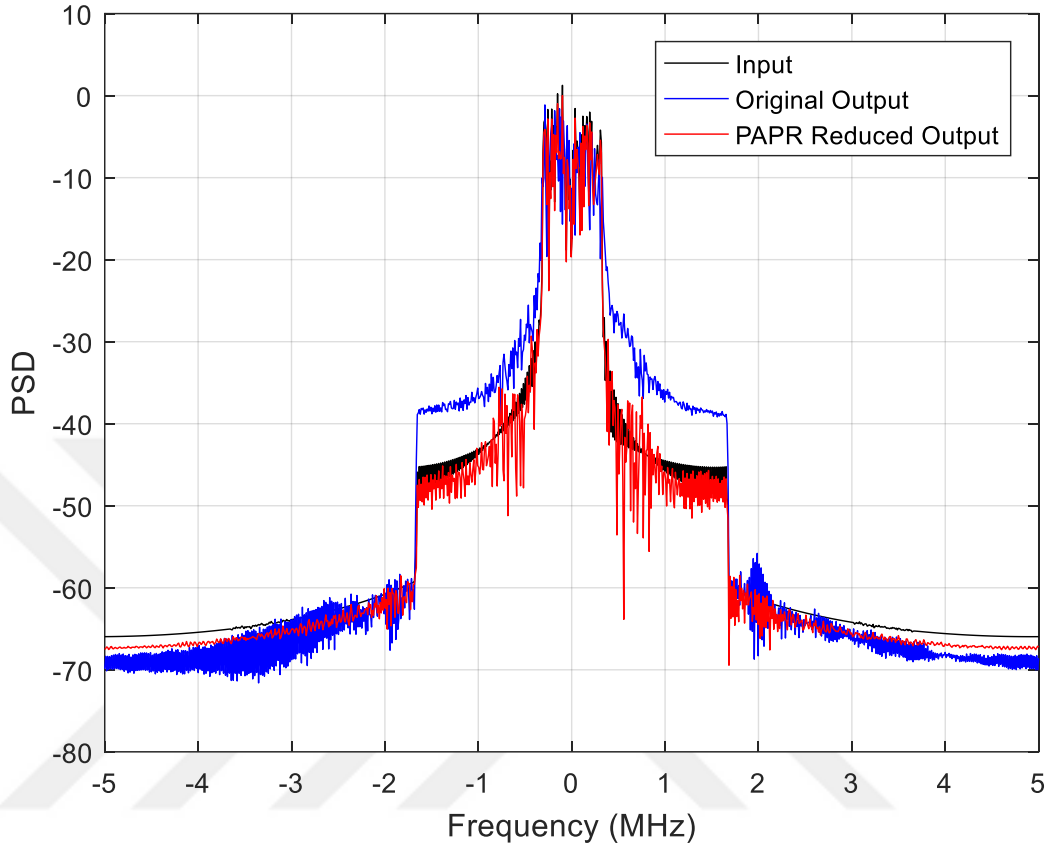

Figure 6.6. PSD plot of input, original and PAPR reduced symbols

Analog to digital conversion and up conversion are carried out on the mezzanine card and the center frequency of the signal is set to 2.4 GHz. To observe the effect of PAPR reduction on nonlinear distortion of the whole system, output of RF mezzanine card and output of PA are measured for both original signal and PAPR reduced signal the results are compared.

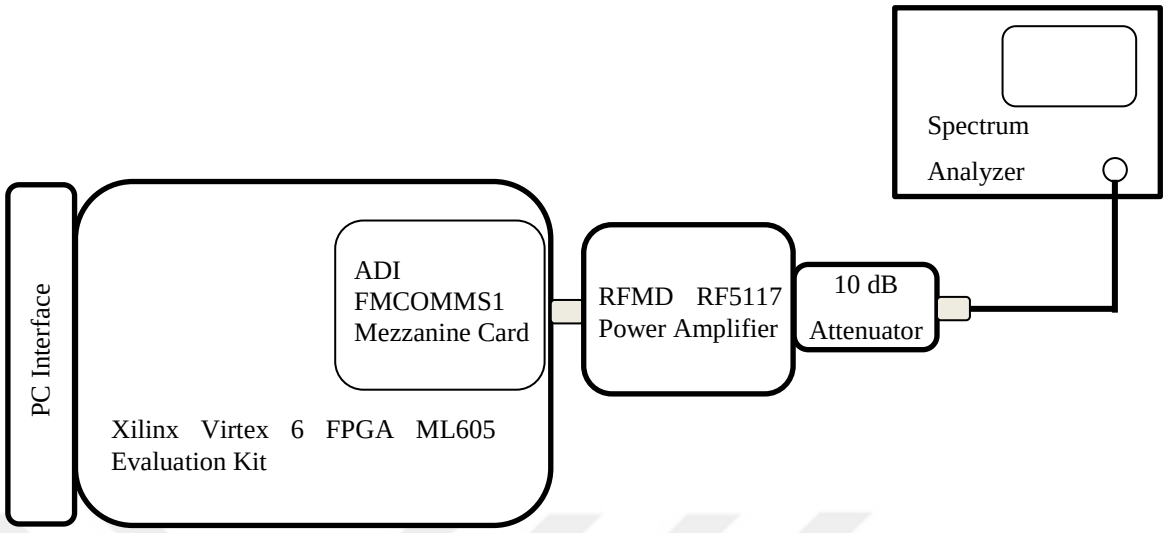

Figure 6.7. Block diagram of SDR

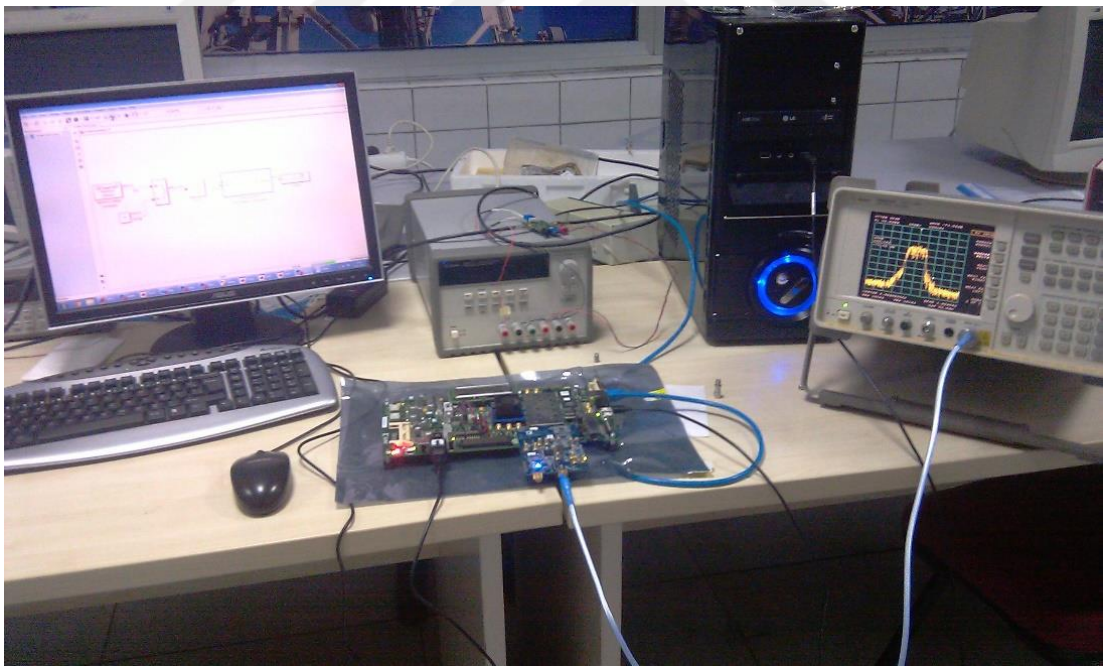

Figure 6.8. Physical appearance of the experiment setup

In Figure 6.9, original signal is measured both at the output of RF mezzanine card and output of PA by using spectrum analyzer. Measurements are carried out within 10 MHz span bandwidth at the 2.4 GHz center frequency. In the figure, lower peak at the center is the output of the RF mezzanine card. To obtain ACPR values, average power in 10 kHz band is measured. As seen in the figure, the signal has ACPR of -30 dBc at 1 MHz from the carrier frequency and this implies that SDR platform induces nonlinear distortion even before the PA. The second and the higher is the signal after the PA. As seen in the figure, PA amplify the RF mezzanine card's output 25 dB and the average peak power is equals to 3 dBm. However, nonlinear distortion is also increased.

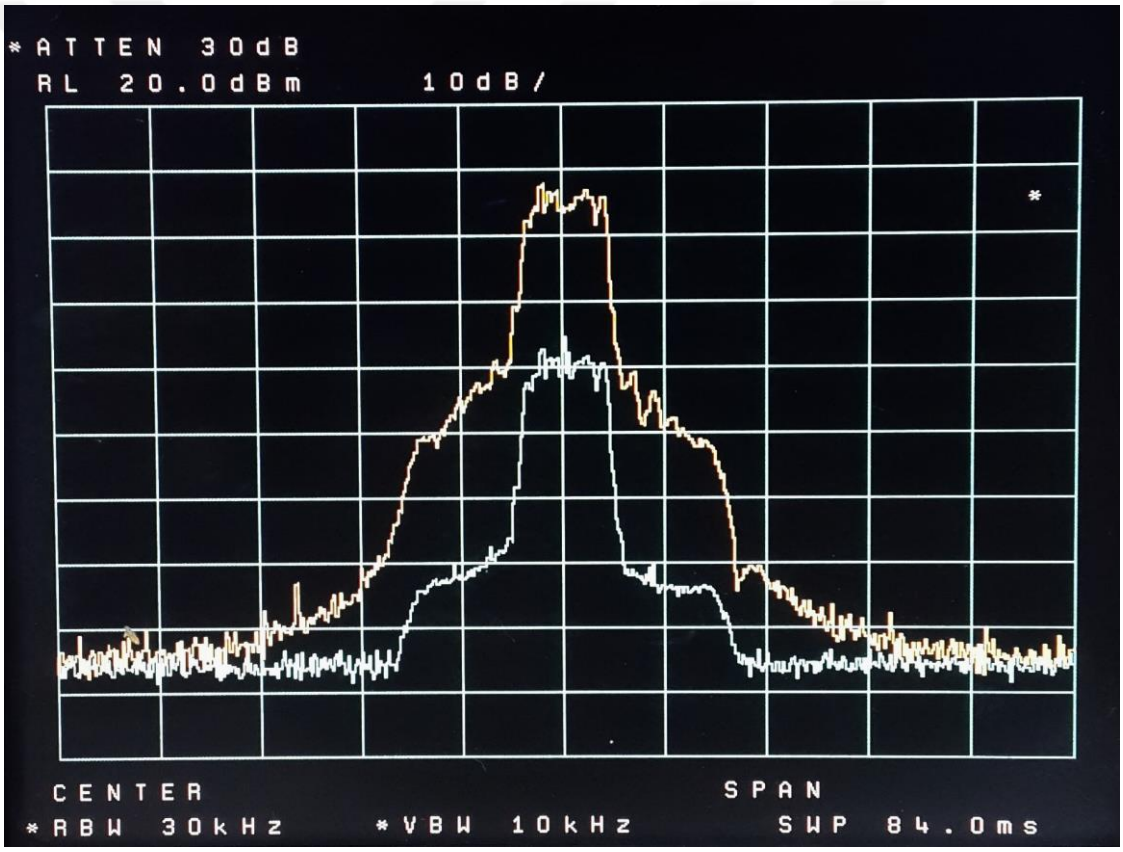

Figure 6.9. Spectrum of SDR output and PA output with original signal

In Figure 6.10, PAPR reduced signal is used to measure the outputs of RF mezzanine card and PA with the same span bandwidth and center frequency as the previous measurement. Also in this figure, the result with lower peak is belongs to the output of RF mezzanine card. However, unlike the previous measurement, ACPR is decreased from -25 dBc to -40 dBc this means that, nonlinear distortion of the SDR platform is decreased. As seen in the figure, signal is amplified by PA 25 dB and average peak power is measured as 3 dBm.

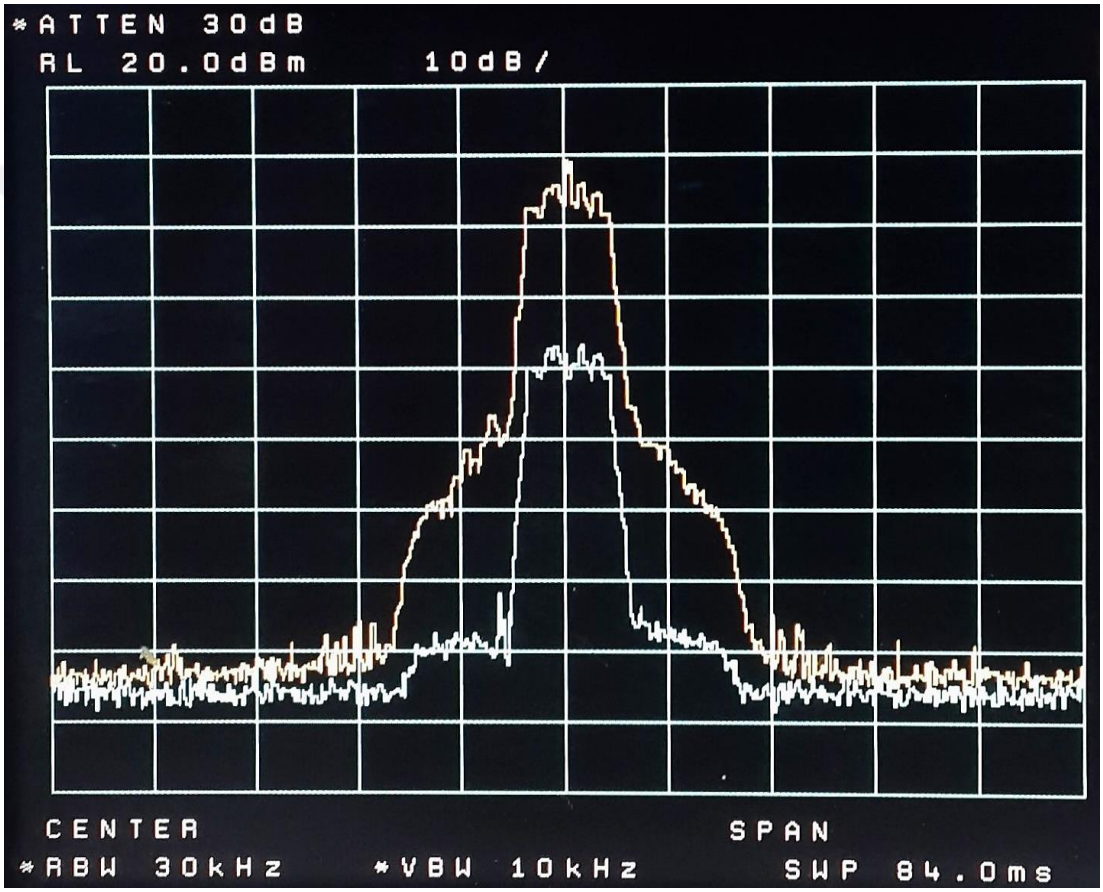

Figure 6.10. Spectrum of SDR output and PA output with PAPR reduced signal

In Figure 6.11, spectrum measurements of original signal and PAPR reduced signals after the PA are given. ACPR is measured for 1 MHz periods and the results given in Table 6.4. As seen in table, ACPR is decreased 15 dB in the band 1 MHz far from carrier frequency. For the other bands, 10 dB and 2 dB improvements are obtained. It is clearly seen that, nonlinear distortion in the adjacent channels is decreased by PAPR reduction.

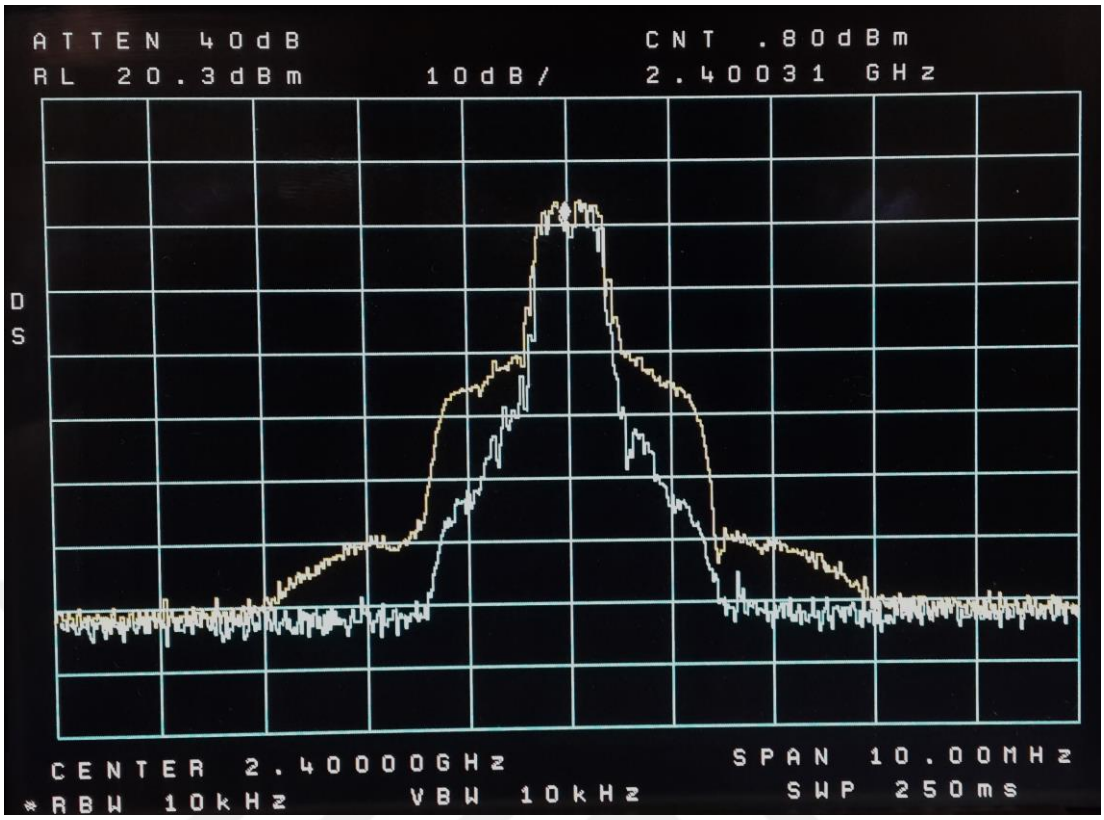

Figure 6.11. Spectrum of OFDM signal with and without PAPR reduction

Table 6.4: Measurement Results of Original and PAPR Reduced Signals

Measurement Interval From Center	Original (dBm)	ACPR (dBc)	PAPR Reduced (dBm)	ACPR (dBc)
-3 MHz	-58	-58	-60	-60
-2 MHz	-50	-50	-60	-60
- 1 MHz	-27	-27	-42	-42
Center	0	-	0	-
+1 MHz	-28	-28	-43	-43
+2 MHz	-51	-51	-60	-60
+3 MHz	-58	-58	-60	-60

CHAPTER 7

CONCLUSION

OFDM systems are highly sensitive to nonlinear distortion because of the high PAPR of OFDM signal. This study presents PAPR reduction by using TI and SA algorithms together. It is the first time these methods are used together and this can be considered as the contribution of this study to the literature. Throughout the studies, it is seen that slight differences may bring drastic changes on PAPR. When only 2 or 3 of 64 tones are changed, PAPR reduces dramatically. Researcher proposed to use TI with searching on created data set or analytical optimization algorithms and this complicates the process. SA algorithm randomly searches the solution space and by imitating the cooling process, narrows the possible solutions.

Firstly, TI and SA techniques are applied with different number of tones. Results show that, increasing number of tones decreases PAPR. However, it increases the average power. According to the results, reduction with TI and SA would be better than common techniques. Secondly, TI and SA techniques are applied with inner threshold, which is set to 6 dB. Results show that, 2 tone injection is not adequate to decrease PAPR but 3, 4, 5 and 6 tone injection processes are successful and the highest PAPR is obtained as 6 dB. It is also seen that, applying an inner threshold decreases the iteration number. This study also shows tradeoffs between number of tones, necessary number of iteration and average power value. The system requirements (time, speed,

bandwidth, value of nonlinear distortion) can be chosen to define how the proposed method will be applied to decrease PAPR on any system.

In this study, OFDM system with PAPR reduction technique is designed and targeted to a SDR platform, which includes FPGA and RF mezzanine card. The output of SDR is wired to a PA. The results of PAPR reduction technique are compared with unmodified result by using spectrum analyzer. ACPR measurements show that, PAPR reduction decreases ACI is caused by nonlinear distortion. It is observed by the experimental results that, PAPR is reduced using the proposed method on a SDR system.

REFERENCES

[1] R. Van Nee, and R. Prasad, OFDM for wireless multimedia communications, Artech House, 2000.

[2] Y. S. Cho, et al. MIMO-OFDM wireless communications with MATLAB. John Wiley & Sons, 2010.

[3] S. Hara, and R. Prasad. Multicarrier techniques for 4G mobile communications. Artech House, 2003.

[4] ETSI EN 300 401 v1.4.1 "Radio Broadcasting Systems; Digital Audio Broadcasting (DAB) to mobile, portable and fixed receivers"

[5] ETSI EN 300 744 V1.6.1, Digital Video Broadcasting (DVB); Framing structure, channel coding, and modulation for digital terrestrial television," Jan. 2009.

[6] 802.11ad-2012 - IEEE Standard for Information technology-Telecommunications and information exchange between systems.

[7] IEEE 802.16™: Broadband Wireless Metropolitan Area Networks (MANs)

[8] Asymmetric digital subscriber line (ADSL) transceivers, G.992.1, ITU.

[9] 3GPP specification: Requirements for further advancements for E-UTRA (LTE Advanced)

[10] J. P Carlos, and N. B. Carvalho. Intermodulation distortion in microwave and wireless circuits. Artech House, 2002.

[11] B. Razavi, RF microelectronics (Vol. 2). New Jersey, Prentice Hall, 2011.

[12] Y. Kim, Y. Yang, S.H. Kang, and B. Kim, "Linearization of 1.85 GHz amplifier using feedback predistortion loop", IEEE MTT-S Int. Microw. Symp. Dig., pp. 1675-1678,1998,

[13] A.K. Ezzeddine, H.A. Hung, and H.C. Huang, “An MMAC C-band FET feedback power amplifier”, IEEE Transactions on Microwave Theory and Techniques 38, pp. 350-357, 1990.

[14] H. Coskun, A. Mutlu, and S. Demir, “A multitone model of complex enveloped signals and its application in feedforward circuit analysis”, IEEE Transactions on Microwave Theory and Techniques 53, pp. 2171-2178, 2005.

[15] D.K. Paul, and G. Parkinson, “A New Approach for the Linearization of a Distributed Amplifier”, Microwave and Optical Technology Letters 46, pp. 15-17, 2005.

[16] C. Ciflikli, A.T. Ozsahin, A.C. Yapici, “Artificial Neural Network Channel Estimation Based on Levenberg-Marquardt for OFDM Systems”, Wireless Personal Communications, vol.51, pp. 221-229, 2009.

[17] L. Ding, G.T. Zhou, D.R. Morgan, Z. Ma, J.S. Kenney, J. Kim, and J.R. Giardina, “A robust digital baseband predistorter constructed using memory polynomials”, IEEE Transactions on Communications, 52, pp. 159-165, 2004.

[18] C. Ciflikci, A.C. Yapıcı, “Genetic algorithm optimization of a hybrid analog/digital predistorter for RF power amplifiers”, Analog Integrated Circuits and Signal Processing, vol. 52, pp. 25-30, 2007.

[19] R. O'neill, and L.B. Lopes. "Envelope variations and spectral splatter in clipped multicarrier signals", Personal, Indoor and Mobile Radio Communications, PIMRC'95. Wireless: Merging onto the Information Superhighway, Sixth IEEE International Symposium on. Vol. 1. IEEE, 1995.

[20] A. Jha, M.S.M. Sher, S.S. Alam, M.T. Hasan, and M.M. Rahman, "Reduction of Peak to Average Power Ratio (PAPR) in Orthogonal Frequency Division Multiplexing (OFDM): A Novel Approach Based on Clipping and Amplification." Computer Sciences and Convergence Information Technology, ICCIT'09. Fourth International Conference on. IEEE, 2009.

[21] K. Bandara, S. Tiwari, and Y. H. Chung. "Novel Nonlinear Companding Transform for Reduced Peak-to-Average Power Ratio in OFDM."Computer, Consumer and Control (IS3C), 2014 International Symposium on. IEEE, 2014.

[22] Y. Wang, et al. "Nonlinear companding transform technique for reducing PAPR of ODFM signals." IEEE Transactions on Consumer Electronics 58.3 (2012): 752-757.

[23] H. Li, T. Jiang, and Y. Zhou, “An improved tone reservation scheme with fast convergence for PAPR reduction in OFDM systems”, IEEE Transactions on Broadcasting, 57(4), 902-906.

[24] J. Tellado, and J. M. Cioffi. "Peak power reduction for multicarrier transmission." IEEE GLOBECOM. Vol. 99. 1998.

[25] N., Jacklin, and Z. Ding, “A linear programming based tone injection algorithm for PAPR reduction of OFDM and linearly precoded systems”, IEEE Transactions on Circuits and Systems I: Regular Papers, 60(7), 1937-1945.

[26] N. Shigei, H. Kumashiro, and H. Miyajima, “Parallel stochastic search for PAPR reduction of OFDM signal”, 2014 Joint 7th International Conference on In Soft Computing and Intelligent Systems (SCIS), and 15th International Symposium on Advanced Intelligent Systems (ISIS), (pp. 317-322). IEEE, 2014.

[27] M. Ohta, Y. Ueda, and K. Yamashita, “PAPR reduction of OFDM signal by neural networks without side information and its FPGA implementation”, “IEEJ Transactions on Electronics, Information and Systems”, vol. 126, pp1296-1303, 2006.

[28] N. Shigei, H. Miyajima, and K. Ozono, "Time-Efficient Genetic Algorithm for Peak Power Reduction of OFDM Signal." Proceedings of the World Congress on Engineering and Computer Science. Vol. 1. San Francisco, USA, 2010.

[29] H. Jun, C. Tellambura, and J. Ge. "Tone injection for PAPR reduction using parallel tabu search algorithm in OFDM systems." IEEE Global Communications Conference (GLOBECOM), 2012.

[30] J.C. Chen, and C.K. Wen, “PAPR reduction of OFDM signals using cross-entropy-based tone injection schemes”, IEEE Signal Processing Letters, 17(8), pp. 727-730, 2010.

[31] C. Tuna, and D.L. Jones, “Tone injection with aggressive clipping projection for OFDM PAPR reduction”. IEEE International Conference on In Acoustics Speech and Signal Processing (ICASSP), pp. 3278-3281, March, 2010.

[32] S.H. Müller, and J.B. Huber, "OFDM with reduced peak-to-average power ratio by optimum combination of partial transmit sequences" Electronics Letters 33.5 pp. 368-369, 1997.

[33] L.J. Jr. Cimini, and N.R. Sollenberger, “Peak-to-average power ratio reduction of an OFDM signal using partial transmit sequences”, IEEE Communications Letters, vol. 4(3), pp. 86-88, 2000.

[34] X. Wang, S. He, and T. Zhu, “A Genetic-Simulated Annealing Algorithm Based on PTS Technique for PAPR Reduction in OFDM System”, IEEE Symposium on In Computer Applications and Communications (SCAC), pp. 120-124, July, 2014.

[35] J. Gao, J. Wang, Z. Xie, and D. Yan, “A modified PTS PAPR reduction algorithm with low computational complexity”, IET 2nd International Conference on Wireless, Mobile and Multimedia Networks (ICWMMN 2008), pp. 333-336, October, 2008.

[36] G. Jing, W. Jinkuan, and X. Zhibin, “A new PTS technique to reduce the peak to average power ration of OFDM system”, International Conference on Microwave and Millimeter Wave Technology, ICMMT Vol. 4, pp. 1953-1956, April, 2008.

[37] T. Jiang, W. Xiang, P.C. Richardson, J. Guo, and G. Zhu, “PAPR reduction of OFDM signals using partial transmit sequences with low computational complexity”, IEEE Transactions on Broadcasting, 53(3), pp. 719-724, 2007.

[38] J.C. Chen, “Partial transmit sequences for PAPR reduction of OFDM signals with stochastic optimization techniques”, IEEE Transactions on Consumer Electronics, 56(3), 1229-1234, 2010.

[39] S.J. Heo, H.S. Noh, J.S. No, D.J. Shin "A modified SLM scheme with low complexity for PAPR reduction of OFDM systems", IEEE 18th International Symposium on Personal, Indoor and Mobile Radio Communications, 2007.

[40] H. Chen, and H. Liang, “Combined selective mapping and binary cyclic codes for PAPR reduction in OFDM systems”, IEEE Transactions on Wireless Communications, vol. 6(10), pp. 3524-3528, 2007.

[41] M. Niranjan, and S. Srikanth. "Adaptive active constellation extension for PAPR reduction in OFDM systems." International Conference on Recent Trends in Information Technology, 2011.

[42] B.S. Krongold, and D.L. Jones, “PAR reduction in OFDM via active constellation extension”, IEEE Transactions on Broadcasting, vol. 49(3), pp. 258-268, 2003.

[43] S. Kirkpatrick, C. D. Gelatt, & M. P. Vecchi, Optimization by simulated annealing, Science, 220(4598), pp. 671-680, 1983.

[44] Wireless Innovation Forum, http://www.wirelessinnovation.org (last visited 15.06.2016)

[45] A.A.M. Saleh and R. Valenzuela. "A statistical model for indoor multipath propagation." IEEE Journal on selected areas in communications 5.2 (1987): 128-137.

[46] P. Nobles and F. Halsall. "Delay spread and received power measurements within a building at 2 GHz, 5 GHz and 17 GHz." Antennas and Propagation, Tenth International Conference on (Conf. Publ. No. 436). Vol. 2. IET, 1997.

[47] S. B. Weinstein, P. M. Ebert, Data Transmission of Frequency Division Multiplexing Using the Discrete Frequency Transform, IEEE Transactions on Communications, COM-19(5), pp. 623–634, October 1971.

[48] M.R.D. Rodrigues, PhD Thesis, “Modeling and Performance Assessment of Communication Systems in Presence of Nonlinearities”, 2002.

[49] Y. Tachwali, W. Barnes, and H. Refai, "Configurable symbol synchronizers for software-defined radio applications," Journal of Network and Computer Applications, vol.32, no.3, pp. 607-615, 2009

[50] H. Zhang, X. Xia, L. J. Cimini, Jr. Fellow, and P. C. Ching, “Synchronization techniques and guardband-configuration scheme for single-antenna vector-OFDM systems,” IEEE Trans. on Wireless Communications, vol. 4, no. 5, pp 2454-2464, 2005.

[51] J.-P. Javaudin, D. Lacroix and A. Rouxel, "Pilot-aided channel estimation for OFDM/OQAM", 57th IEEE Semiannual Vehicular Technology Conference, Vol. 3. pp. 1581-1585, 2003.

[52] T. Jiang, and Yiyan Wu. "An overview: peak-to-average power ratio reduction techniques for OFDM signals." IEEE Transactions on broadcasting 54.2 (2008): 257.

[53] J. G. Proakis, Intersymbol interference in digital communication systems. John Wiley & Sons, Inc., 2003.

[54] S. Shepherd, J. Orriss, and S. Barton. "Asymptotic limits in peak envelope power reduction by redundant coding in orthogonal frequency-division multiplex modulation." IEEE Transactions on Communications 46.1 (1998): 5-10.

[55] R. Van Nee, and Arnout De Wild. "Reducing the peak-to-average power ratio of OFDM." Vehicular technology conference, 1998. VTC 98. 48th IEEE. Vol. 3. IEEE, 1998.

[56] T. Jiang, et al. "Derivation of PAPR distribution for OFDM wireless systems based on extreme value theory." IEEE Transactions on Wireless Communications 7.4 (2008): 1298-1305.

[57] P. Wong, and B. Pejcinovic. "The influence of model parameters on accurate IMD simulations in HBTs." Electronics, Circuits and Systems, 2001. ICECS 2001. The 8th IEEE International Conference on. Vol. 1. IEEE, 2001.

[58] K. Hyunchul, and J. S. Kenney. "Behavioral modeling of RF power amplifiers considering IMD and spectral regrowth asymmetries." Microwave Symposium Digest, 2003 IEEE MTT-S International. Vol. 2. IEEE, 2003.

[59] J. A. García, et al. "Accurate nonlinear resistive FET modeling for IMD calculations." Microwave Conference, 1998. 28th European. Vol. 2. IEEE, 1998.

[60] J. P. Aikio,, J. Vuolevi, and T. Rahkonen. "Detailed Analysis of IMD of HBT PA Based on VBIC Model." 2006 European Microwave Integrated Circuits Conference. IEEE, 2006.

[61] A.A.M Saleh,., "Frequency-independent and frequency-dependent nonlinear models of TWT amplifiers," IEEE Trans. Communications, vol. COM-29, pp.1715-1720, November 1981.

[62] A. Ghorbani, and M. Sheikhan, "The effect of Solid State Power Amplifiers (SSPAs) Nonlinearities on MPSK and M-QAM Signal Transmission", Sixth Int'l Conference on Digital Processing of Signals in Comm., 1991, pp. 193-197.

[63] C. Rapp, "Effects of HPA-Nonlinearity on a 4-DPSK/OFDM-Signal for a Digitial Sound Broadcasting System", in Proceedings of the Second European Conference on Satellite Communications, Liege, Belgium, Oct. 22-24, 1991, pp. 179-184.

[64] J. Tellado, Multicarrier modulation with low PAR: applications to DSL and wireless. Vol. 587. Springer Science & Business Media, 2006.

[65] Xilinx, Virtex 6 User Manual, http://www.xilinx.com/publications/prod_mktg/ml605_product_brief.pdf, (last visited 10.07.2016)

[66] Analog Device, AD- FMCOMMS1 User Manual
http://www.analog.com/en/evaluation/eval-fmcomms/eb.html (last visited 5.07.2016)

[67] RFMD, 5117 PA User Manual

http://www.rfmd.com/store/downloads/dl/file/id/29574/rf5117_data_sheet.pdf (last visited 05.07.2016)

[68] J. Mitola, "The software radio architecture." IEEE Communications magazine 33.5 (1995): 26-38.

[69] Mathworks, HDL Coder http://www.mathworks.com/products/hdl-coder/index.html (last visited 10.07.2016)

[70] Mathworks, MATLAB and Simulink Hardware Support for SDR http://www.mathworks.com/discovery/sdr (last visited 10.07.2016)